

A Two-stage Image Segmentation Method Using a Convex Variant of the Mumford-Shah Model and Thresholding

Raymond H. Chan

Department of Mathematics
Chinese University of Hong Kong

Joint work with

Xiaohao Cai (Kaiserslautern Technical University)

Hongfei Yang (University of Nottingham)

Tieyong Zeng (Hong Kong Baptist University)



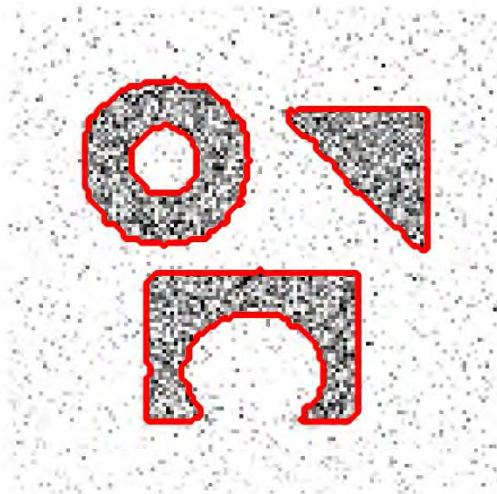
*Bob's Birthday Workshop
Nov 17-18, 2013*

*Supported by
HKRGC*

Aim: One Method to Segment Different Images



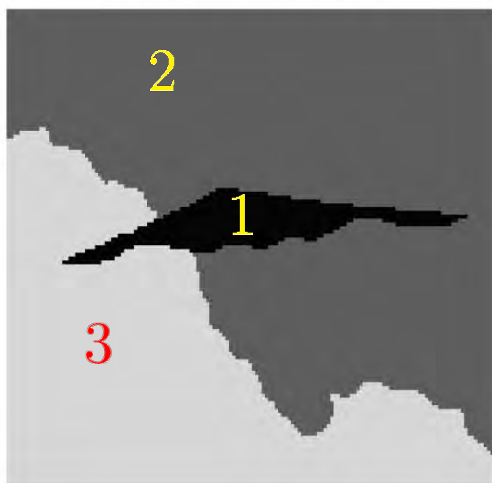
anti-mass



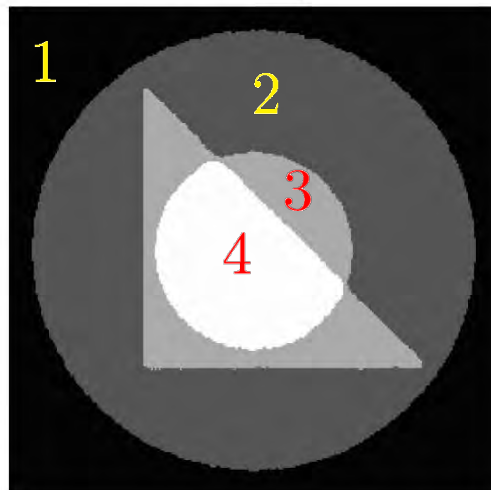
noisy



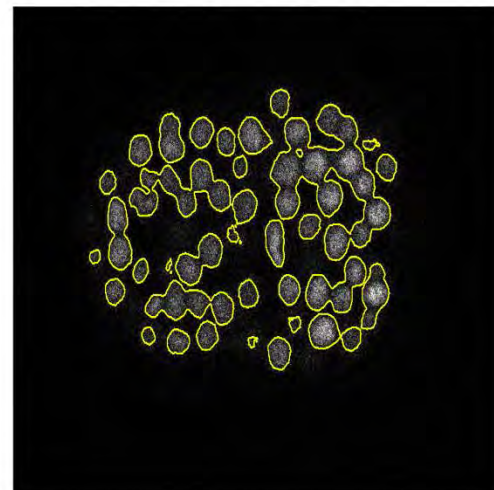
tubular



3-phase

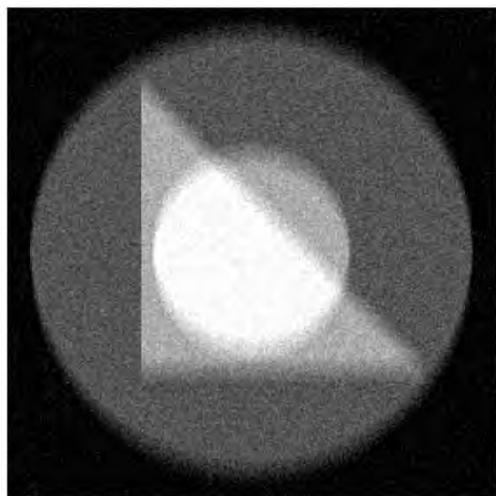


4-phase blurry

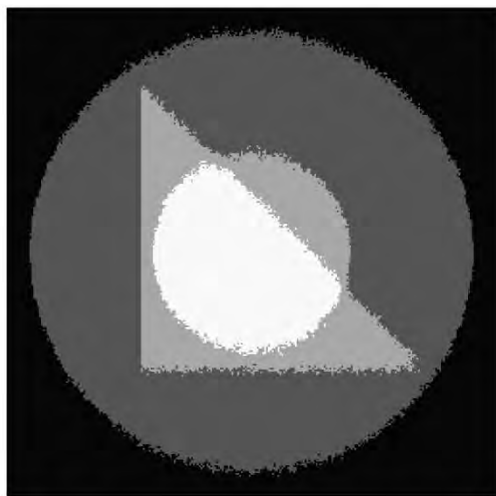


non-Gaussian

Multiphase Segmentation for Blurry Image



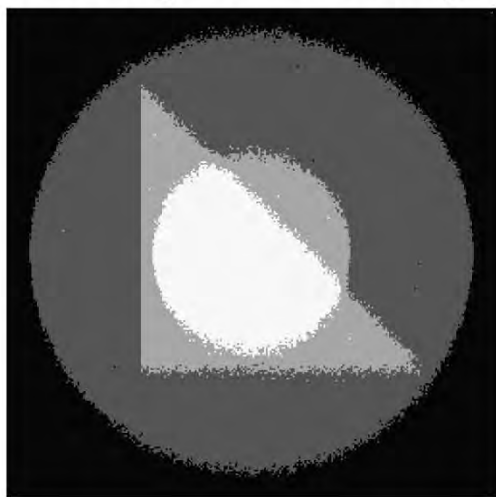
Noisy & blurry



Li *et al.* (10)



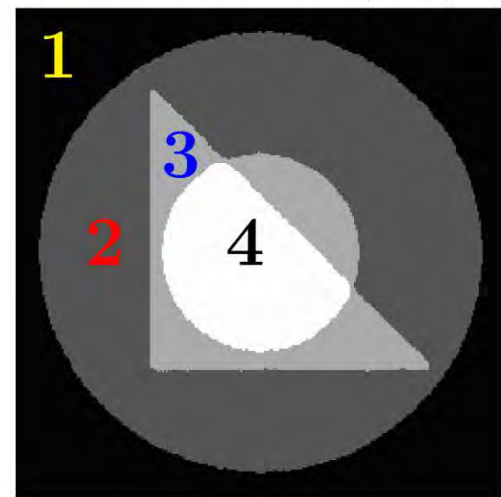
Yuan *et al.* (10)



Sandberg *et al.* (10)



Steidl *et al.* (12)

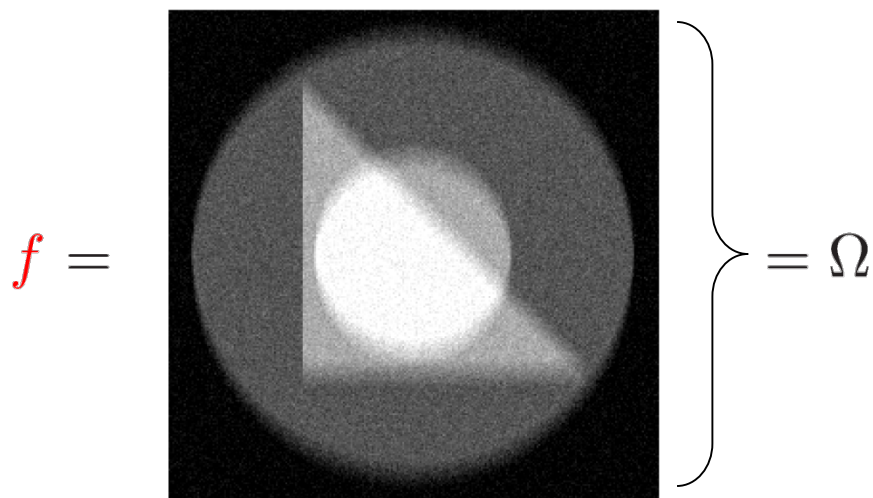


Our result

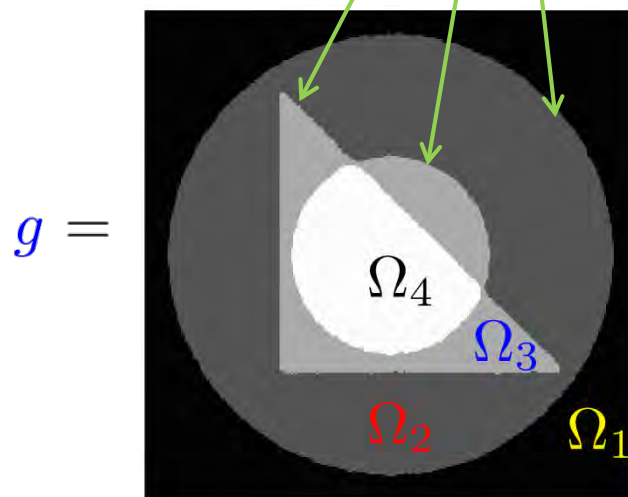
- 1. Mumford-Shah Model**
- 2. Our Two-stage Image Segmentation Method**
- 3. Experimental Results**
- 4. Extensions to Other Noise Models**
- 5. Conclusions**

Problem Setting and Notation

Given a noisy and blurry image f ,



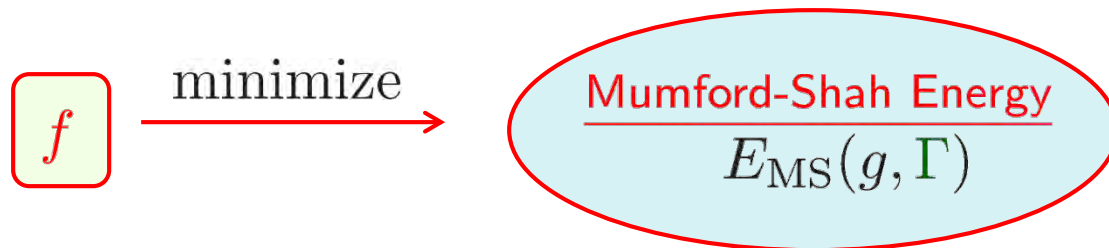
want a K -phase
segmentation :



$$K = 4$$

$$\begin{aligned} \Omega \setminus \Gamma &= \cup_i \Omega_i, \\ g &= c_i \text{ in } \Omega_i, \\ i &= 1, 2, 3, 4 \end{aligned}$$

Mumford-Shah Model (1989)



$$\frac{\lambda}{2} \int_{\Omega} (f - g)^2 dx + \frac{\mu}{2} \int_{\Omega \setminus \Gamma} |\nabla g|^2 dx + \text{Length}(\Gamma)$$

Data fidelity:
control g not far
away from f

Regularization:
impose smoothness
of g on $\Omega \setminus \Gamma$

Regularization:
require boundary
 Γ be short

Mumford-Shah Model (1989)

Mumford-Shah Energy
 $E_{\text{MS}}(g, \Gamma)$



$$\frac{\lambda}{2} \int_{\Omega} (f - g)^2 dx$$

+

$$\frac{\mu}{2} \int_{\Omega \setminus \Gamma} |\nabla g|^2 dx$$

+

Length(Γ)

Nonconvex:
due to the
edge term Γ

Finding Good Approximation of M-S Model

Mumford-Shah Energy
 $E_{\text{MS}}(g, \Gamma)$

Find a good approximation



$$\frac{\lambda}{2} \int_{\Omega} (f - g)^2 dx$$

+

$$\frac{\mu}{2} \int_{\Omega \setminus \Gamma} |\nabla g|^2 dx$$

+

Length(Γ)

- Pock and Cremers, *et al.* (2009):
A 128×128 image on a Tesla C1060 GPU machine requires 600 seconds.

Simplifying Mumford-Shah Model

Mumford-Shah Energy
 $E_{\text{MS}}(g, \Gamma)$

Simplify it:
 $\nabla g \equiv 0$ on $\Omega \setminus \Gamma$

$$\frac{\lambda}{2} \int_{\Omega} (f - g)^2 dx$$

+

$$\frac{\mu}{2} \int_{\Omega \setminus \Gamma} |\nabla g|^2 dx$$

+

$$\text{Length}(\Gamma)$$

\equiv
 $= 0$

Multiphase Chan-Vese Model (02)
(minimizer \hat{g} is **piecewise constant**):

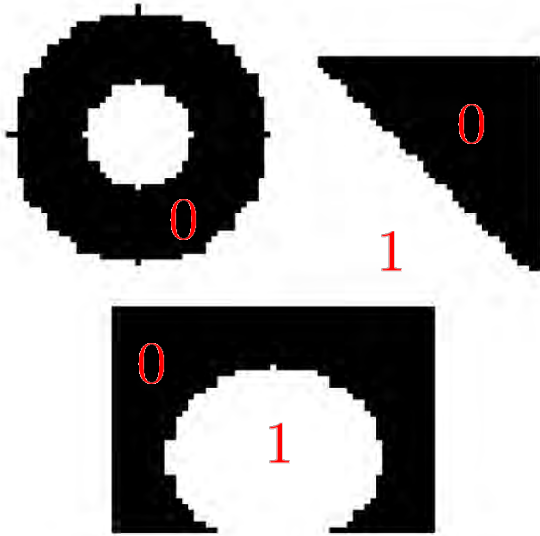
$$E_{\text{MS}}(\{c_i\}, \Gamma) = \frac{\lambda}{2} \sum_{i=1}^K \int_{\Omega_i} (f - c_i)^2 + \text{Length}(\Gamma)$$

2-phase
 \longrightarrow

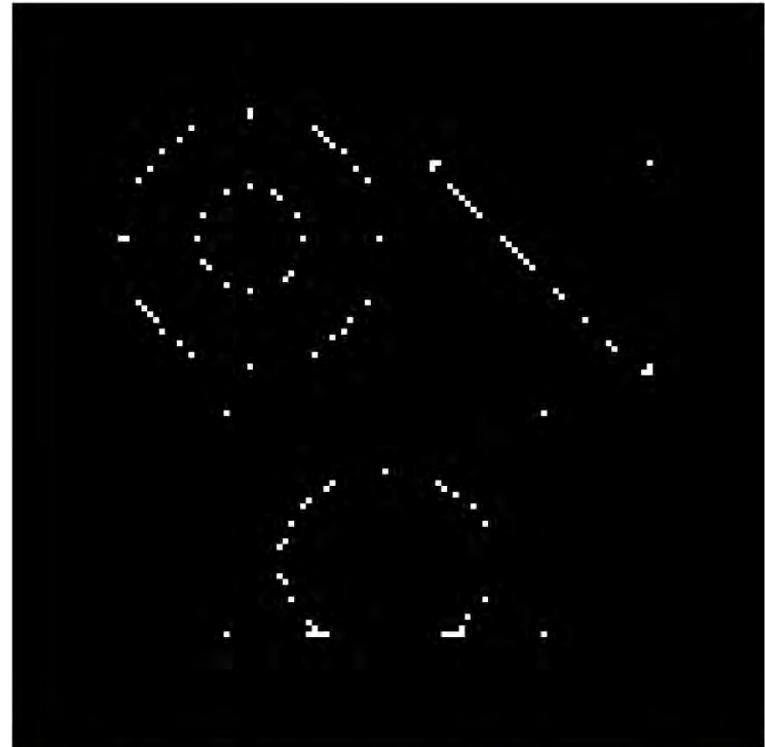
ACWE (01):
 $\Omega \setminus \Gamma = \Omega_1 \cup \Omega_2$
 $\hat{g} = c_i$ in Ω_i

1. Mumford-Shah Model
2. **Our Two-stage Image Segmentation Method**
3. Experimental Results
4. Extensions to Other Noise Models
5. Conclusions

Our Motivation



(a): True binary image

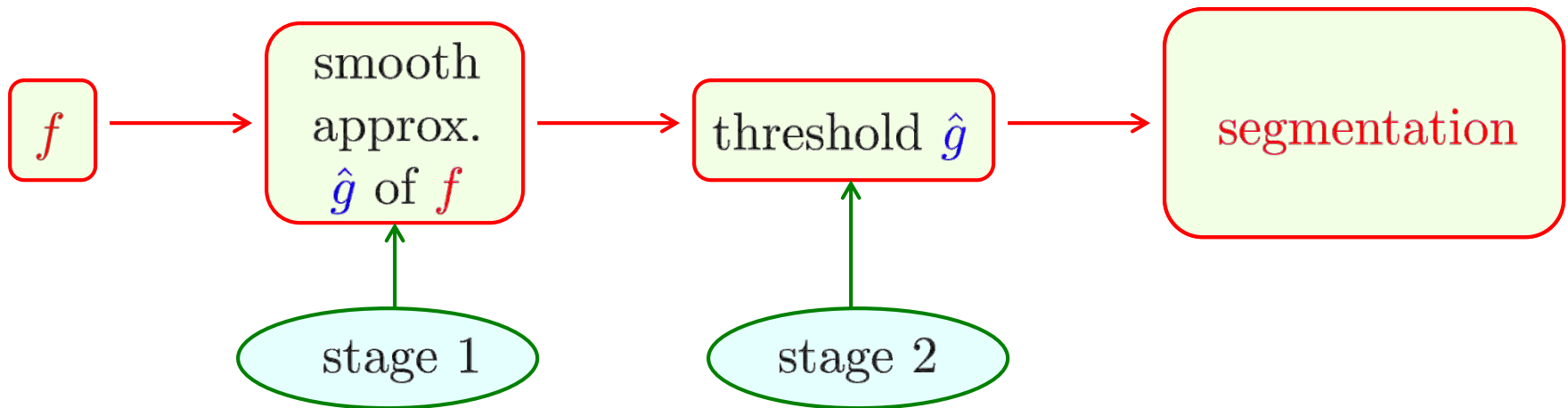


(d): Difference of (a) and (c)
(nonzero pixel values
only at the boundary)

Aim in Segmentation

Chan-Vese: Get a piecewise constant approximation \hat{g} of f

Our idea:



Cai, C., Morigi, and Sgallari, Vessel segmentation in medical imaging using a tight-frame based Algorithm, *SIAM J. Imaging Sci.*, (2013)

Stage One: Convex Variant of the M-S Model

Mumford-Shah Energy
 $E_{\text{MS}}(g, \Gamma)$

Restrict:
 $g \in W^{1,2}(\Omega)$



$$\frac{\lambda}{2} \int_{\Omega} (f - g)^2 dx$$

+

$$\frac{\mu}{2} \int_{\Omega \setminus \Gamma} |\nabla g|^2 dx$$

+

Length(Γ)

Lemma 1



$$\frac{\lambda}{2} \int_{\Omega} (f - g)^2 dx$$

+

$$\frac{\mu}{2} \int_{\Omega} |\nabla g|^2 dx$$

+

$$\int_{\Omega} |\nabla g| dx$$

Approx.
 Thm. 2 ⇕



Convex M-S Energy
 $E(g)$

Stage One: Lemma 1

Lemma 1

If $g \in W^{1,2}(\Omega)$ and Γ is a closed curve with Lebesgue measure $m(\Gamma) = 0$, then

$$\int_{\Gamma} |\nabla g|^2 dx = 0.$$

Proof: Since $g \in W^{1,2}(\Omega)$, we have $\nabla g \in L^2(\Omega)$. Because of $m(\Gamma) = 0$, we get $\int_{\Gamma} |\nabla g|^2 dx = 0$ immediately.

Stage One: Convex Variant of the M-S Model

Mumford-Shah Energy
 $E_{\text{MS}}(g, \Gamma)$

Restrict:
 $g \in W^{1,2}(\Omega)$



$$\frac{\lambda}{2} \int_{\Omega} (f - g)^2 dx$$

+

$$\frac{\mu}{2} \int_{\Omega \setminus \Gamma} |\nabla g|^2 dx$$

+

Length(Γ)

Lemma 1



Approx.
Thm. 2



$$\frac{\lambda}{2} \int_{\Omega} (f - g)^2 dx$$

+

$$\frac{\mu}{2} \int_{\Omega} |\nabla g|^2 dx$$

+

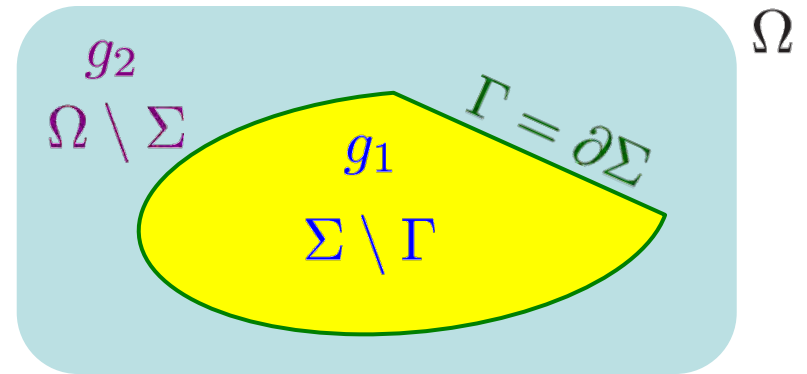
$$\int_{\Omega} |\nabla g| dx$$



Convex M-S Energy
 $E(g)$

Stage One: Theorem 2 (for 2-phase)

For $K = 2$,
let $\Sigma = \overline{\text{Inside}(\Gamma)}$,
 $g_1 \in W^{1,2}(\Sigma \setminus \Gamma)$, and
 $g_2 \in W^{1,2}(\Omega \setminus \Sigma)$.



Rewrite the Mumford-Shah model as:

$$\begin{aligned} E_{\text{MS}}(\Sigma, g_1, g_2) &= \frac{\lambda}{2} \int_{\Sigma \setminus \Gamma} (f - g_1)^2 dx + \frac{\mu}{2} \int_{\Sigma \setminus \Gamma} |\nabla g_1|^2 dx \\ &+ \frac{\lambda}{2} \int_{\Omega \setminus \Sigma} (f - g_2)^2 dx + \frac{\mu}{2} \int_{\Omega \setminus \Sigma} |\nabla g_2|^2 dx \\ &+ \boxed{\text{Length}(\Gamma)}. \end{aligned}$$

Even if g_1 and g_2 are given, finding Σ is still **non-convex**.

Stage One: Theorem 2 (for 2-phase)

Theorem 2 (cf. T. Chan, Esedoglu, and Nikolova (06))

Given g_1 and $g_2 \in W^{1,2}(\Omega)$, a global minimizer Σ for MS model $E_{\text{MS}}(\Sigma; g_1, g_2)$ can be found by solving the convex minimization:

$$\min_{0 \leq g \leq 1} \left\{ \int_{\Omega} \left[\frac{\lambda}{2} (f - g_1)^2 + \frac{\mu}{2} |\nabla g_1|^2 - \frac{\lambda}{2} (f - g_2)^2 - \frac{\mu}{2} |\nabla g_2|^2 \right] g(x) + \int_{\Omega} |\nabla g| \right\},$$

for \tilde{g} and setting $\Sigma = \{x : \tilde{g}(x) \geq \rho\}$ for a.e. $\rho \in [0, 1]$.

- Σ is determined by thresholding \tilde{g}
- $\text{Length}(\Gamma) \approx \int_{\Omega} |\nabla g|$
- equal if \tilde{g} is binary and piecewise constant

Mumford-Shah Model for SBV

When restricted to special functions of bounded variations ([Ambrosio-Giorgi, 88]), Mumford-Shah model becomes

$$\min_{g \in SBV} \left\{ \frac{\lambda}{2} \int_{\Omega} |f - g|^2 + \frac{\mu}{2} \int_{\Omega \setminus J_g} |\nabla g|^2 + \mathcal{H}^1(J_g) \right\},$$

where J_g is the jump set of g and \mathcal{H}^1 is the Hausdorff measure of dimension 1.

- See [Cagnetti & Scardia, 08] and [Stekalovskiy *et al.*, 12]
- If g is binary and piecewise-constant, then $J_g = \Gamma$ and

$$\mathcal{H}^1(J_g) = \text{Length}(\Gamma) = \int_{\Omega} |\nabla g|$$

Mumford-Shah Model for Binary Disk

Consider segmenting a binary disk $f = a\chi_{B(0,1)}$.

The M-S model has two solutions:

(i) $\Gamma = \partial B(0, 1)$ and g minimizes

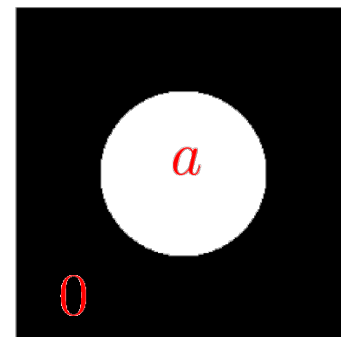
$$\min_g \left\{ \frac{\lambda}{2} \int_{\Omega} |f - g|^2 + \int_{\Omega} |\nabla g| \right\},$$

(ii) $\Gamma = \emptyset$ and g minimizes

$$\min_g \left\{ \frac{\lambda}{2} \int_{\Omega} |f - g|^2 + \frac{\mu}{2} \int_{\Omega} |\nabla g|^2 \right\}.$$

Both solutions can be reproduced by our model:

$$E(g) = \frac{\lambda}{2} \int_{\Omega} (f - g)^2 dx + \frac{\mu}{2} \int_{\Omega} |\nabla g|^2 dx + \int_{\Omega} |\nabla g| dx$$



Stage One: Convex Variant of the M-S Model

Mumford-Shah Energy

$$E_{\text{MS}}(g, \Gamma)$$



$$\frac{\lambda}{2} \int_{\Omega} (f - g)^2 dx$$

+

$$\frac{\mu}{2} \int_{\Omega \setminus \Gamma} |\nabla g|^2 dx$$

+

$$\text{Length}(\Gamma)$$



$$\frac{\lambda}{2} \int_{\Omega} (f - g)^2 dx$$

+

$$\frac{\mu}{2} \int_{\Omega} |\nabla g|^2 dx$$

+

$$\int_{\Omega} |\nabla g| dx$$



Convex M-S Energy

$$E(g)$$

Stage One: Extension to Blurred Problems

Convex M-S Energy
 $E(g)$

stage 1



$$\frac{\lambda}{2} \int_{\Omega} (f - g)^2 dx$$

+

$$\frac{\mu}{2} \int_{\Omega} |\nabla g|^2 dx$$

+

$$\int_{\Omega} |\nabla g| dx$$

extendable to blurred
image with blur \mathcal{A}

$$\frac{\lambda}{2} \int_{\Omega} (f - \mathcal{A}g)^2 dx$$

+

$$\frac{\mu}{2} \int_{\Omega} |\nabla g|^2 dx$$

+

$$\int_{\Omega} |\nabla g| dx$$

Stage One: Unique Minimizer

Our *convex* variant of the Mumford-Shah model is:

$$E(g) = \frac{\lambda}{2} \int_{\Omega} (f - \mathcal{A}g)^2 dx + \frac{\mu}{2} \int_{\Omega} |\nabla g|^2 dx + \int_{\Omega} |\nabla g| dx$$

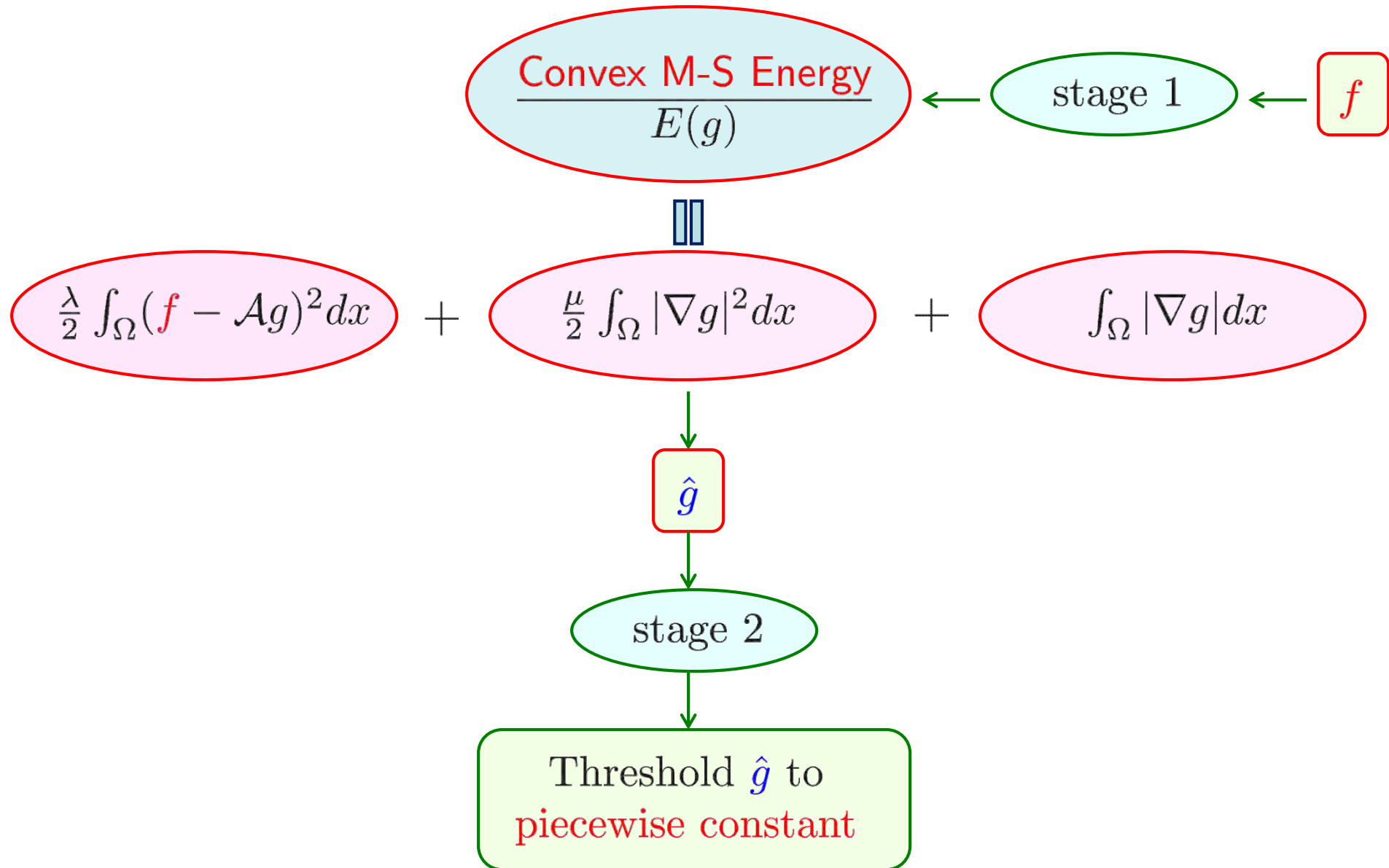
Its discrete version is:

$$\frac{\lambda}{2} \|f - \mathcal{A}g\|_2^2 + \frac{\mu}{2} \|\nabla g\|_2^2 + \|\nabla g\|_1$$

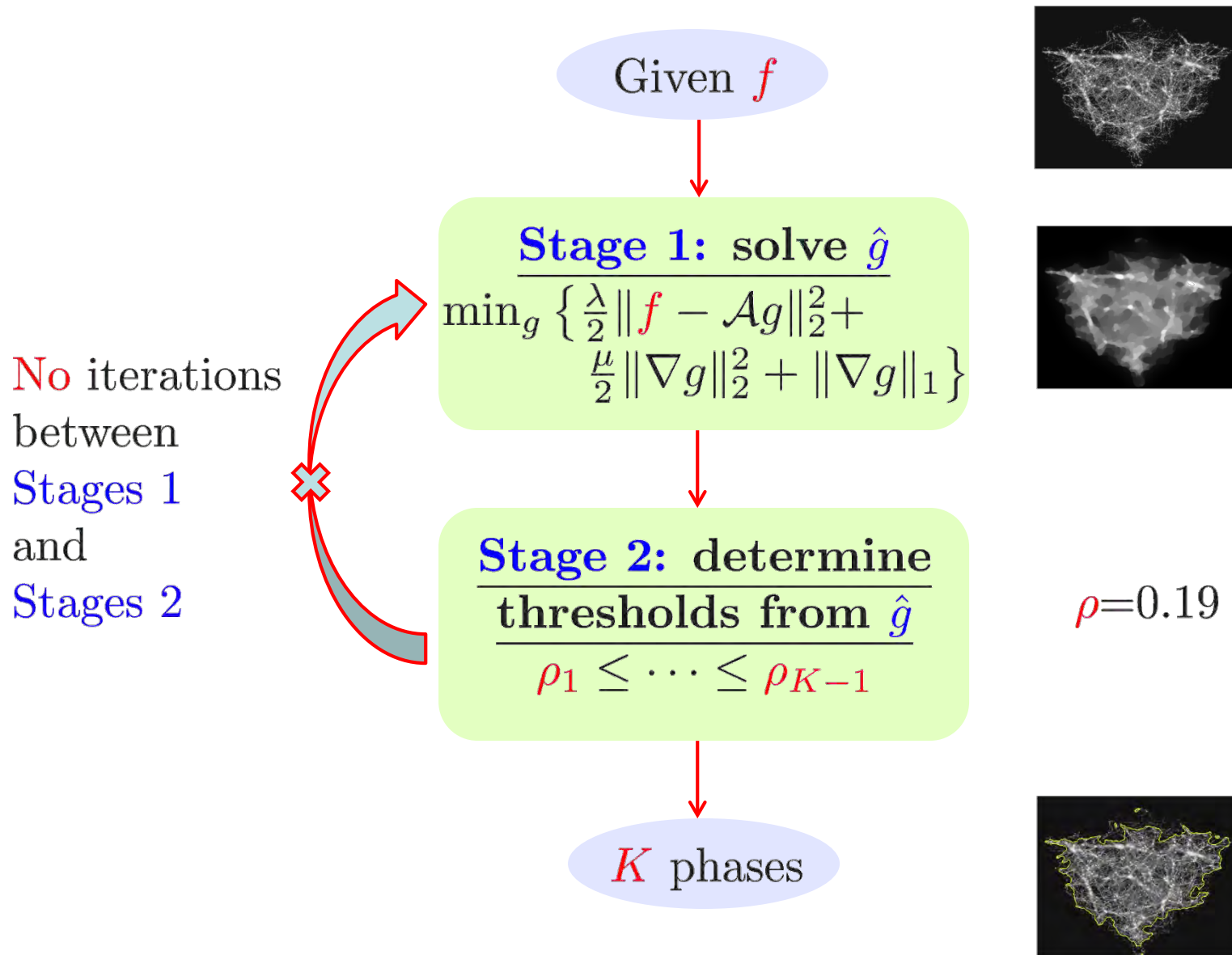
Theorem 3

Let Ω be a bounded connected open subset of \mathbb{R}^2 with a Lipschitz boundary. Let $\text{Ker}(\mathcal{A}) \cap \text{Ker}(\nabla) = \{0\}$ and $f \in L^2(\Omega)$, where \mathcal{A} is a bounded linear operator from $L^2(\Omega)$ to itself. Then $E(g)$ has a *unique minimizer* $g \in W^{1,2}(\Omega)$.

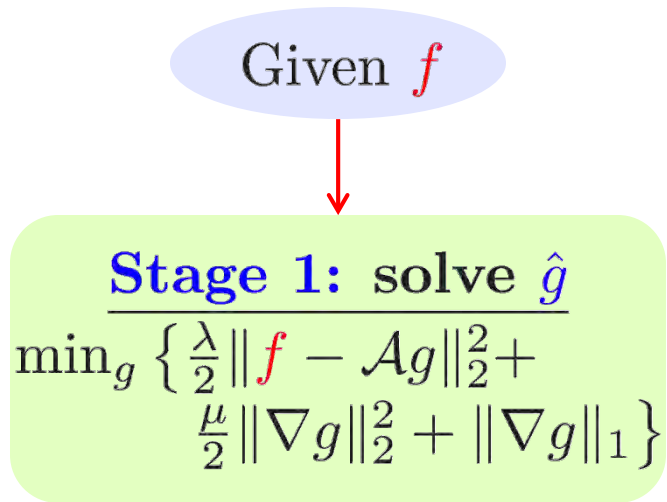
Stage Two: Thresholding



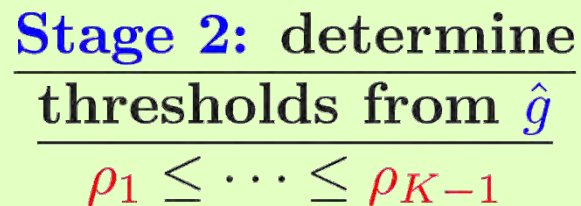
Our Two-stage Segmentation Algorithm



Numerical Aspects: Stage One



Split-Bregman (ADMM)
(Goldstein and Osher, 09);
Augmented Lagrangian
(Tai, *et. al.*, 09);
Chambolle-Pock method
(Chambolle and Pock, 10)
Etc.



K phases

Numerical Aspects: Stage One

Split-Bregman method for solving our model

$$\min_g \left\{ \underbrace{\frac{\lambda}{2} \|f - \mathcal{A}g\|_2^2 + \frac{\mu}{2} \|\nabla g\|_2^2}_{F(g)} + \|\nabla g\|_1 \right\}.$$

Note that $F(g)$ is quadratic in g .

Idea is to separate the g 's in $F(g)$ and $\|\nabla g\|_1$. Set

$$\begin{cases} d_x = \nabla_x g, \\ d_y = \nabla_y g. \end{cases}$$

Numerical Aspects: Stage One

Solve:

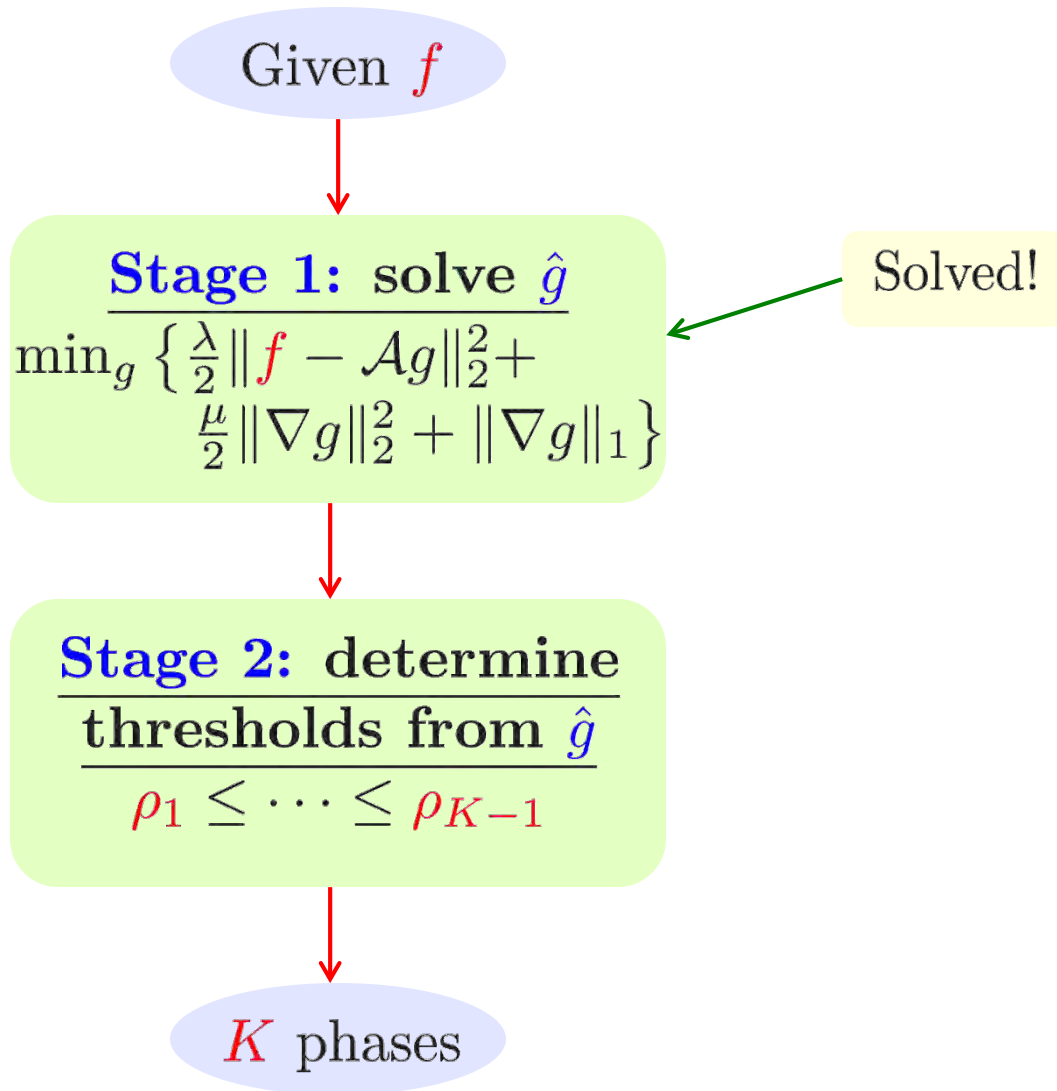
$$\begin{aligned} & \min_{g, d_x, d_y} \left\{ F(g) + \|(d_x, d_y)\|_1 \right\} \\ \text{s.t.} \quad & d_x = \nabla_x g, d_y = \nabla_y g \end{aligned}$$

Split-Bregman iteration:

$$\begin{aligned} (g^{k+1}, d_x^{k+1}, d_y^{k+1}) &= \operatorname{argmin}_{g, d_x, d_y} \left\{ F(g) + \|(d_x, d_y)\|_1 \right. \\ &\quad \left. + \frac{\sigma}{2} \|d_x - \nabla_x g - b_x^k\|_2^2 + \frac{\sigma}{2} \|d_y - \nabla_y g - b_y^k\|_2^2 \right\}, \end{aligned}$$

$$b_x^{k+1} = b_x^k + (\nabla_x g^{k+1} - d_x^{k+1}), \quad b_y^{k+1} = b_y^k + (\nabla_y g^{k+1} - d_y^{k+1}).$$

Numerical Aspects: Stage One



Numerical Aspects: Stage Two

Given f

Stage 1: solve \hat{g}

$$\min_g \left\{ \frac{\lambda}{2} \|f - \mathcal{A}g\|_2^2 + \frac{\mu}{2} \|\nabla g\|_2^2 + \|\nabla g\|_1 \right\}$$

Stage 2: determine thresholds from \hat{g}

$$\rho_1 \leq \dots \leq \rho_{K-1}$$

K phases

Automatic way to determine thresholds by **K-means**

1. Segment the histogram of \hat{g} into K clusters, and compute the mean value of each cluster:

$$m_1 \leq m_2 \leq \dots \leq m_K.$$

2. Define $(K - 1)$ thresholds:

$$\rho_i = \frac{m_i + m_{i+1}}{2}, \quad i = 1, \dots, K - 1.$$

Numerical Aspects: Stage Two

Given f

Stage 1: solve \hat{g}

$$\min_g \left\{ \frac{\lambda}{2} \|f - \mathcal{A}g\|_2^2 + \frac{\mu}{2} \|\nabla g\|_2^2 + \|\nabla g\|_1 \right\}$$

Stage 2: determine thresholds from \hat{g}

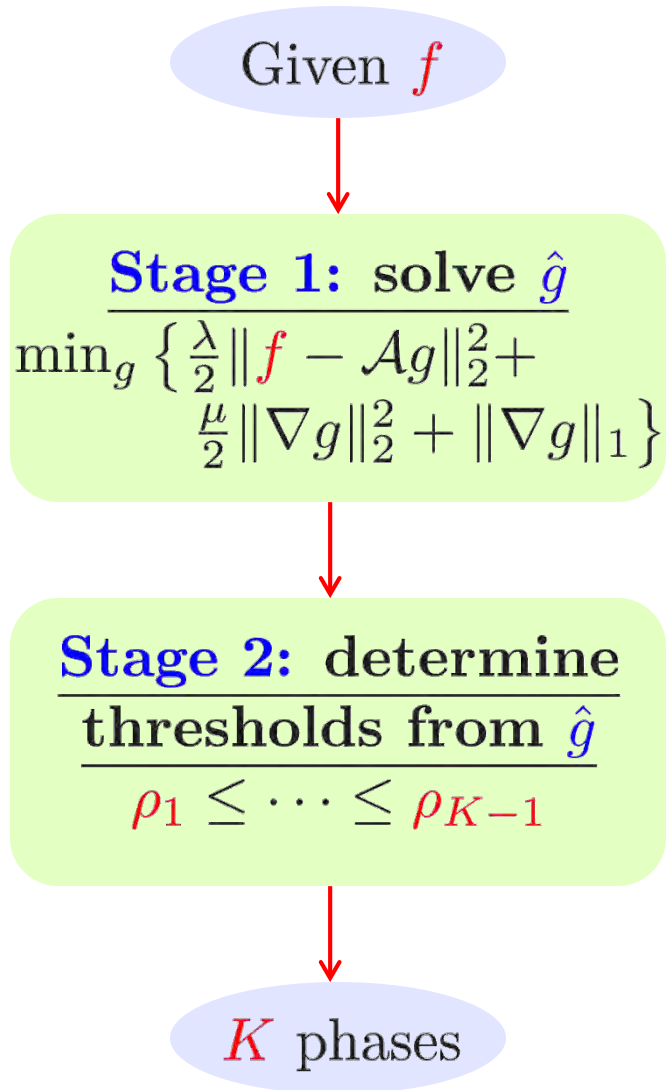
$$\rho_1 \leq \dots \leq \rho_{K-1}$$

K phases

Other Ways

1. Choose by the user: ρ^U .
2. Two-phase: $\rho^M = \text{mean}(\hat{g})$.

Advantages of the 2-Stage Method

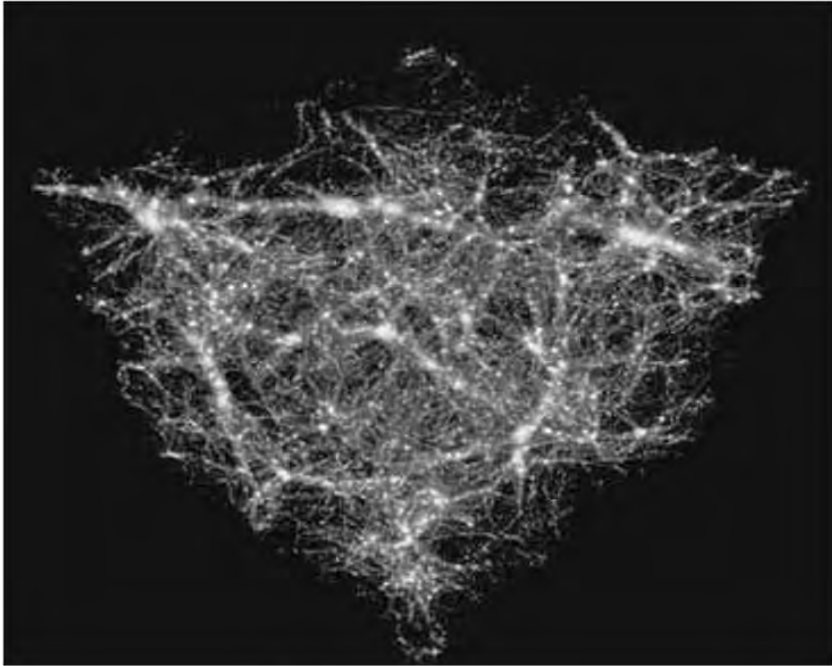


Advantages

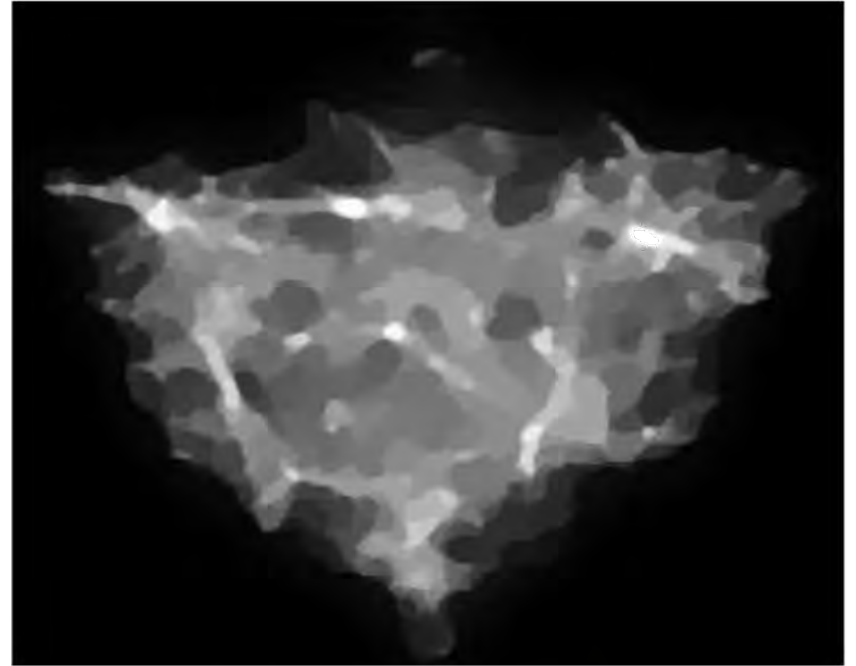
- Stage 1 model for finding \hat{g} is convex
- Stage 2 uses the same \hat{g} when thresholds ρ_i or K change (No need to recompute g)
- No need to fix K at the very beginning
- Easily adapted to blurry and noisy images

1. Mumford-Shah Model
2. Our Two-stage Image Segmentation Method
3. Experimental Results
 - a. Two-Phase Segmentation
 - b. Multi-Phase Segmentation
4. Extensions to Other Noise Models
5. Conclusions

Anti-mass Image: Stage 1 Solution

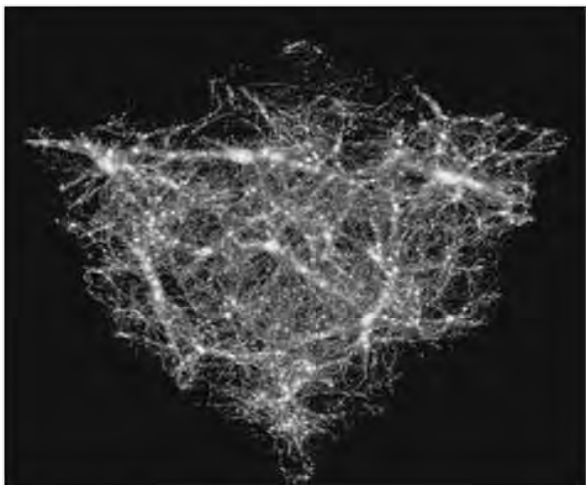


Given image

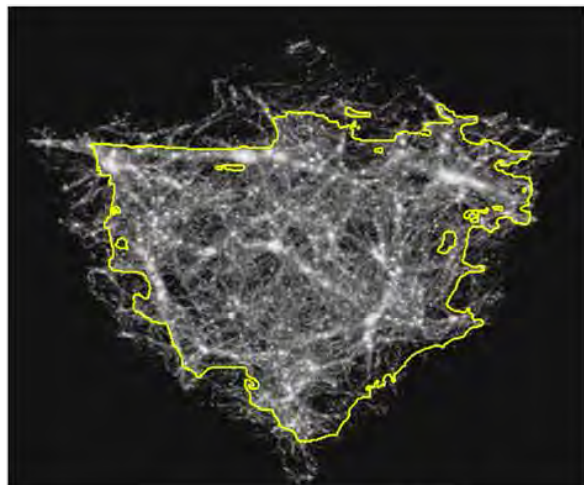


Our solution \hat{g}

Anti-mass Image: Results Comparison



Given image



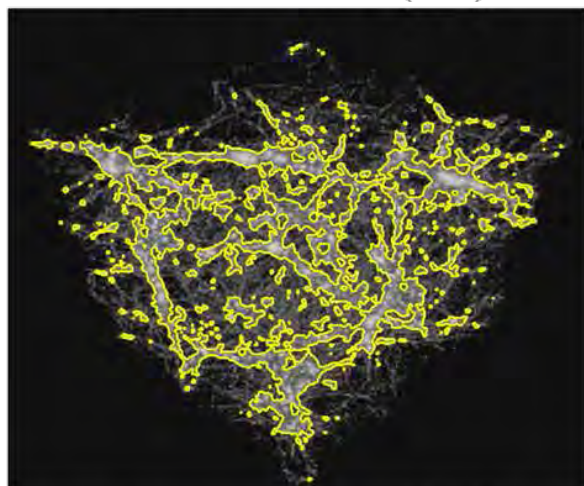
Chan-Vese (01)



Our: $\rho^M = 0.1898$



Dong *et al.* (10)



Yuan *et al.* (10)



Our: $\rho_1 = 0.2669$

Anti-mass Image: *Our Results*



$$\rho^M = 0.1898$$



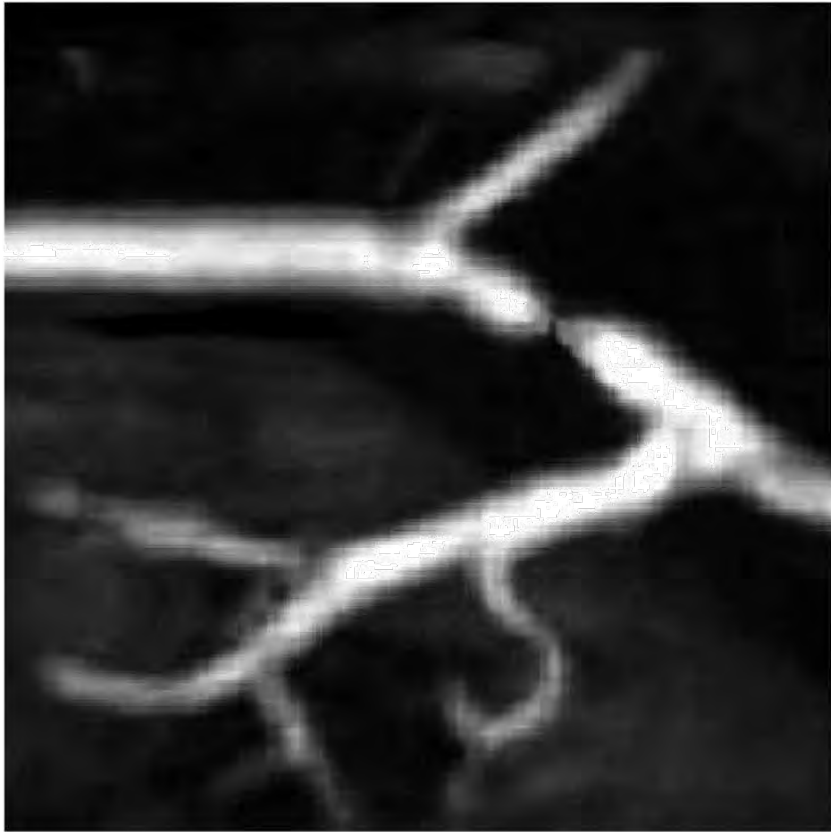
$$\rho^U = 0.2$$



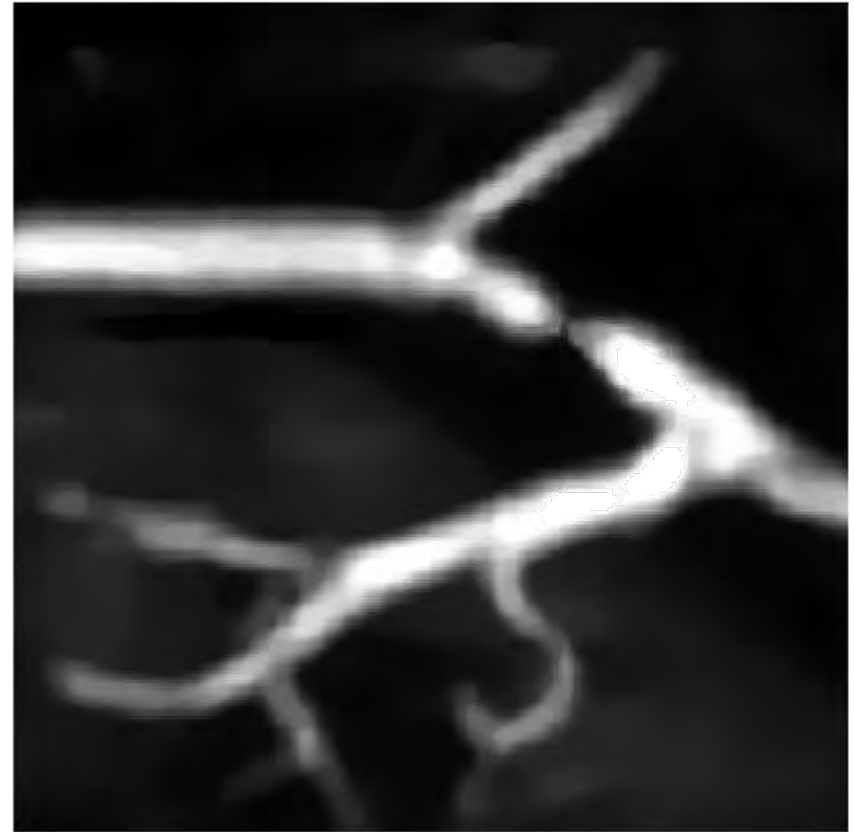
$$\rho_1 = 0.2669$$

Different thresholds give different meaningful segmentation results. **No need to solve** the convex model again when thresholds changed.

Tubular Image: Stage 1 Solution

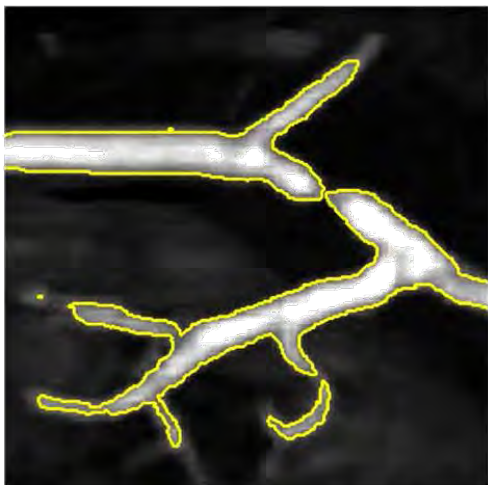


Given image



Our solution \hat{g}

Tubular Image: Results Comparison



Chan-Vese (01)



Yuan *et al.* (10)



$\rho_1 = 0.4019$



Dong *et al.* (10)

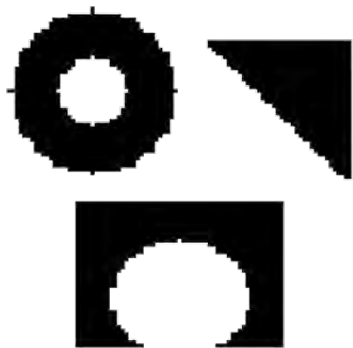


Cai *et al.* (13)

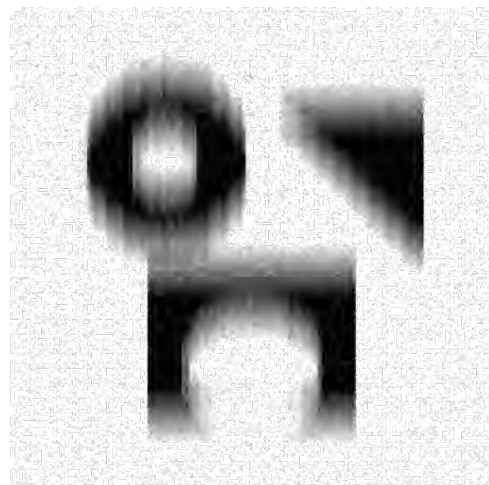


$\rho^M = 0.1760$

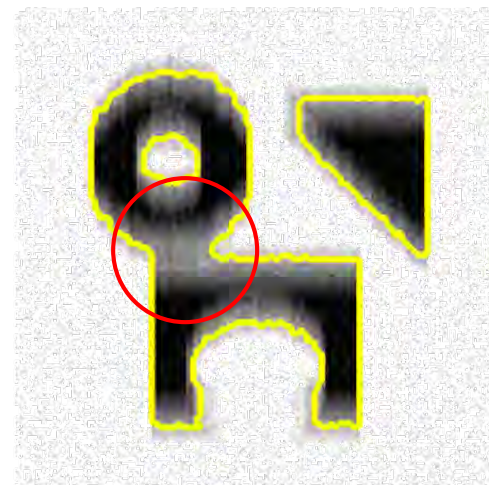
Motion Blurred and Noisy Image



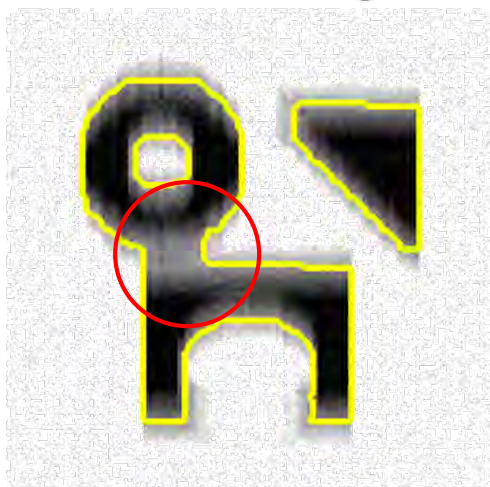
Clean image



Given blurred image



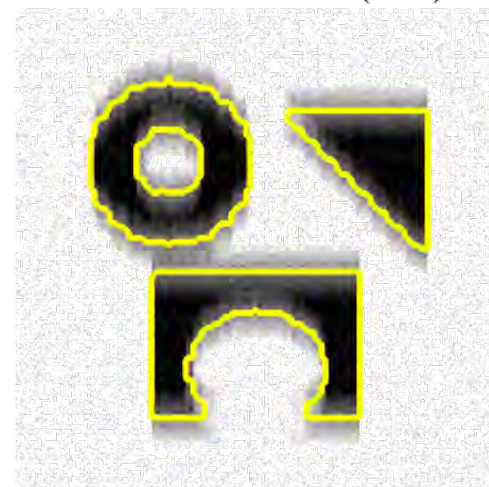
Chan-Vese (01)



Dong *et al.* (10)

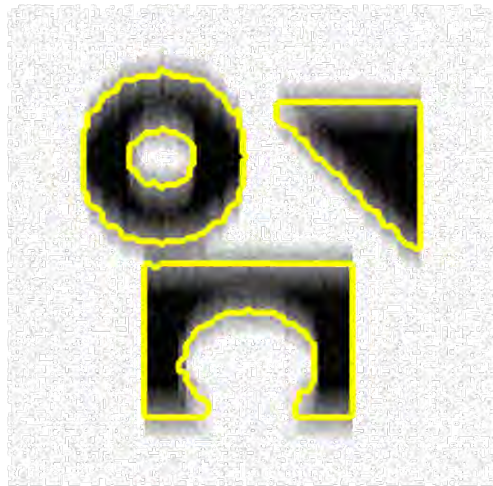


Yuan *et al.* (10)

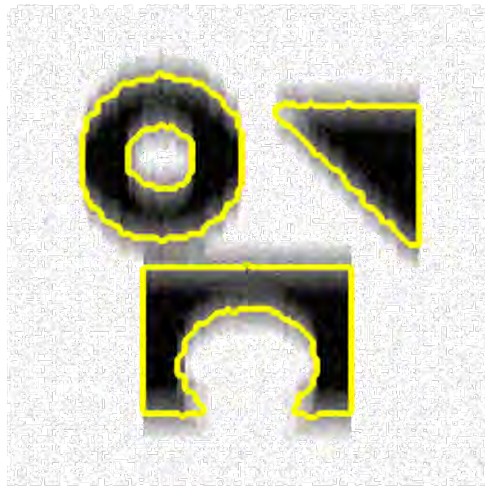


$\rho_1 = 0.5048$

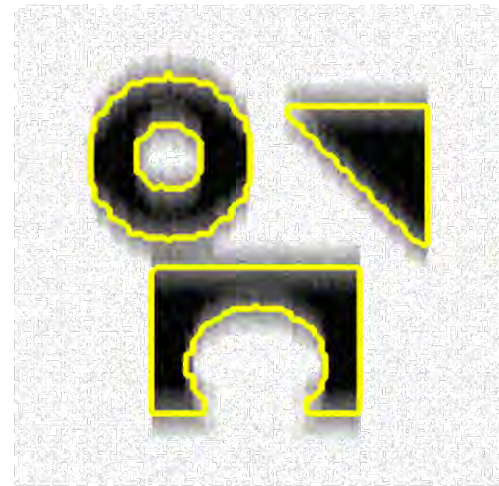
Motion Blurred and Noisy Image



$$\rho^M = 0.7661$$



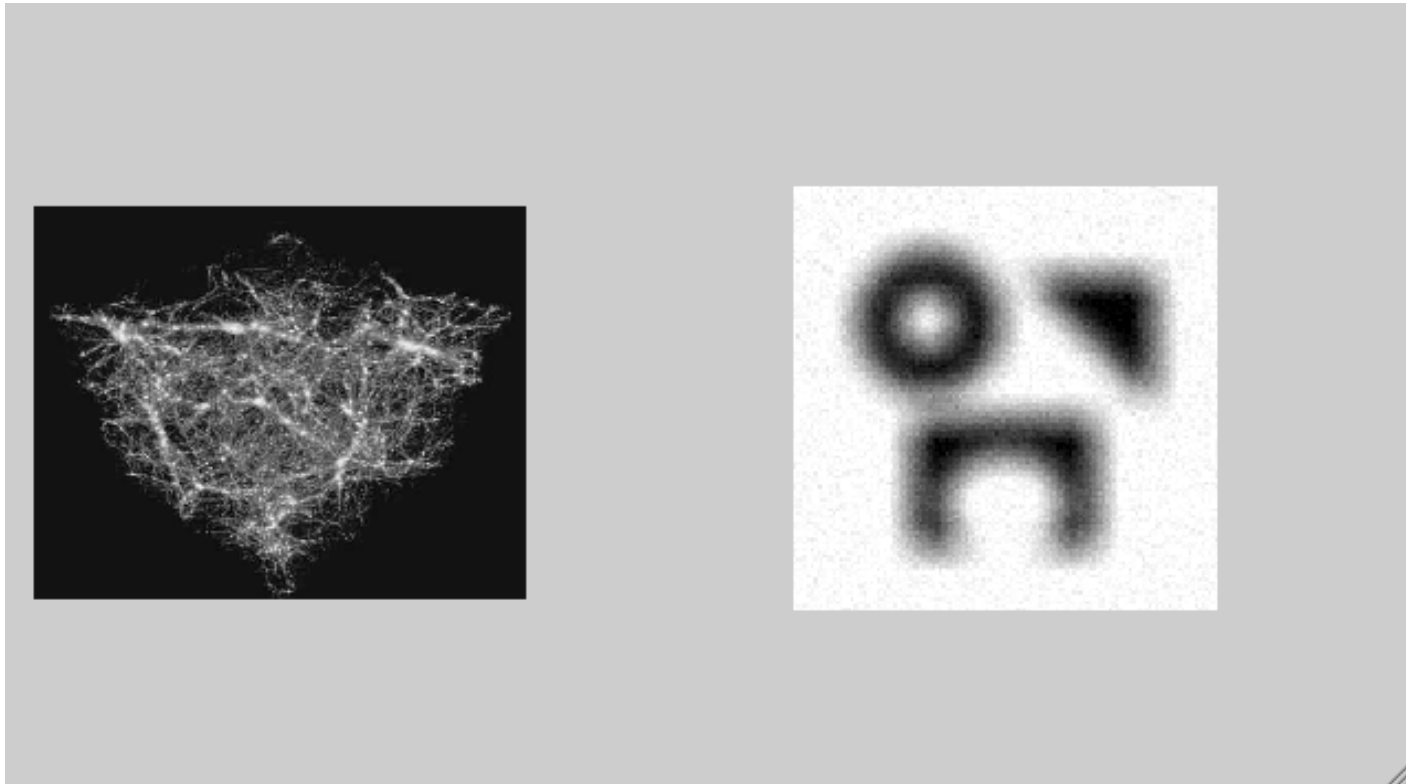
$$\rho^U = 0.6$$



$$\rho_1 = 0.5048$$

Robust with respect to the thresholds chosen

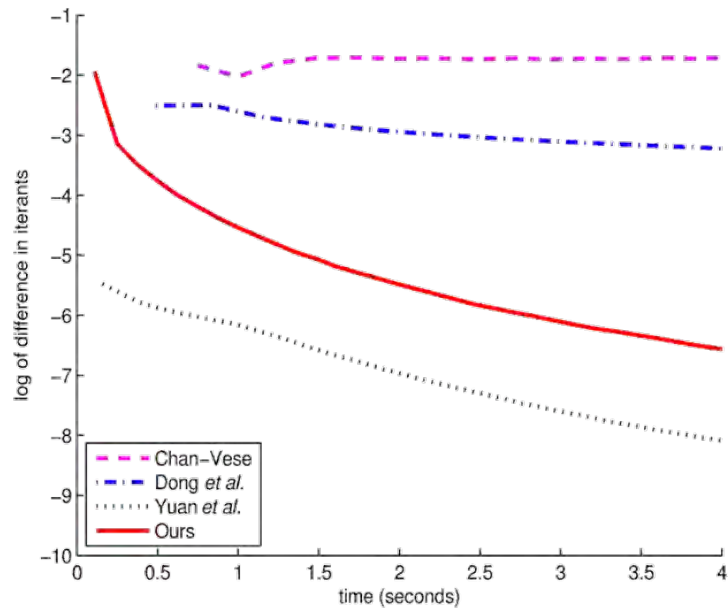
Segmentation Changes with Threshold



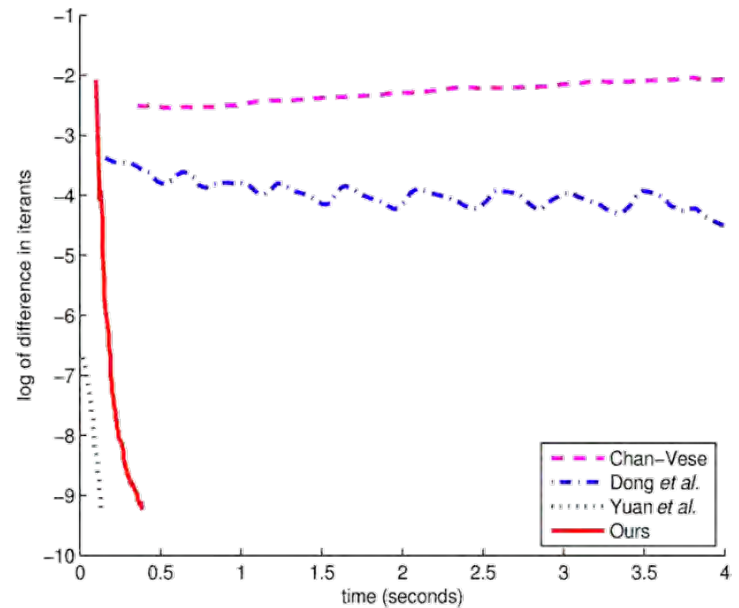
Γ changes as ρ changes. But no need to solve for \hat{g} again.

Convergence History

Log of difference in iterates versus CPU time



Anti-mass image



Motion blurred and noisy image

Our method is very **stable**.

CPU Time

Two-phase: iteration numbers and CPU time in second

Example	C-V (01)		Dong (10)		Yuan (10)		Our method	
	iter.	time	iter.	time	iter.	time	iter.	time
Anti-mass	1000	263.73	300	83.82	64	6.01	172	18.38
Tubular	1000	76.62	300	32.17	18	0.37	115	3.03
Motion	1300	28.19	300	10.18	20	0.09	52	1.13

Our method is faster than others except Yuan's, but our segmentation results are better.

1. Mumford-Shah Model
2. Our Two-stage Image Segmentation Method
3. Experimental Results
 - a. Two-Phase Segmentation
 - b. Multi-Phase Segmentation**
4. Extensions to Other Noise Models
5. Conclusions

Three-phase Segmentation



Given image



Li *et al.* (10)



Sandberg *et al.* (10)



Yuan *et al.* (10)

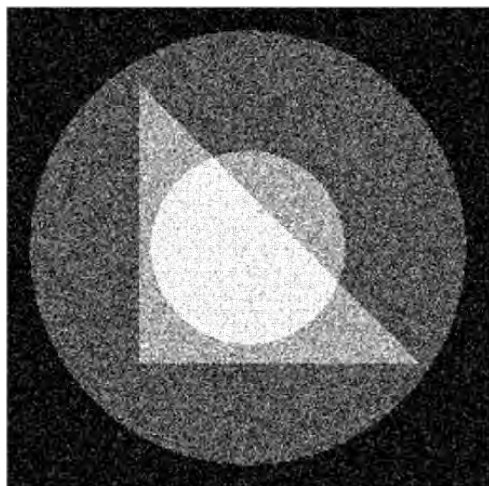


Our solution \hat{g}

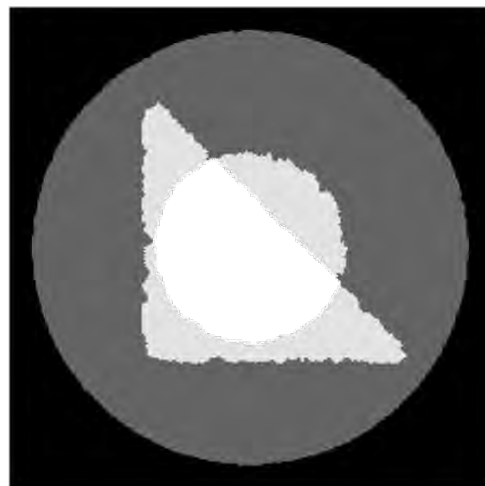


Our 3 phases from \hat{g}
using K-means ρ_i

Four-phase Segmentation: Noisy image



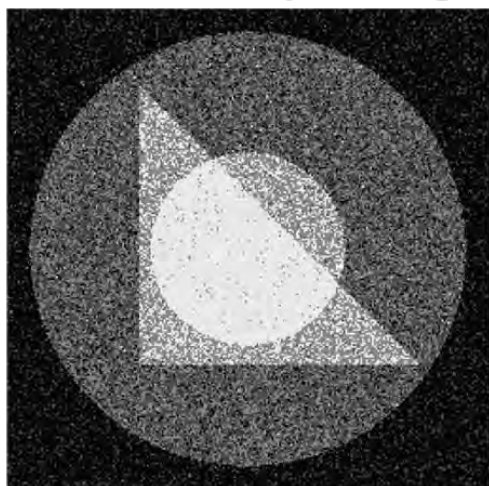
Given noisy image



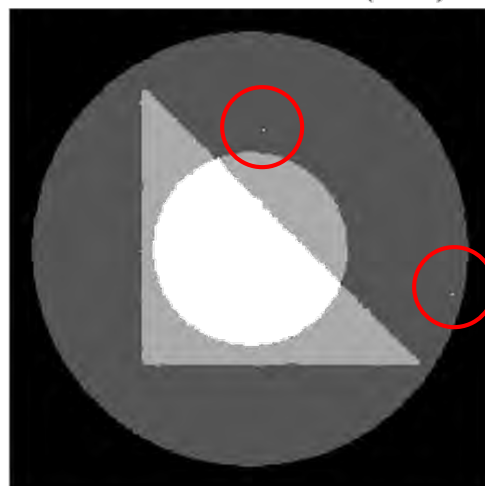
Yuan *et al.* (10)



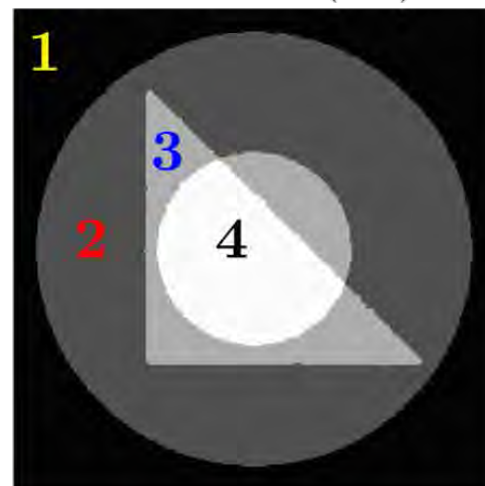
Li *et al.* (10)



Sandberg *et al.* (10)

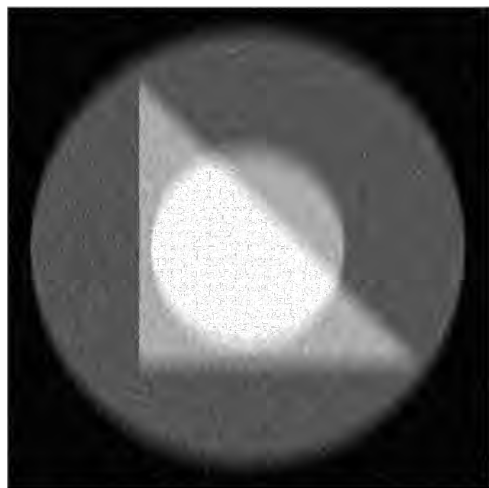


Steidl *et al.* (12)

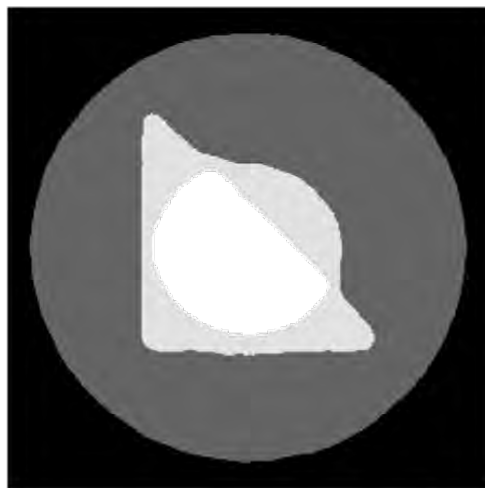


Our 4 phases from \hat{g}
using K-means ρ_i

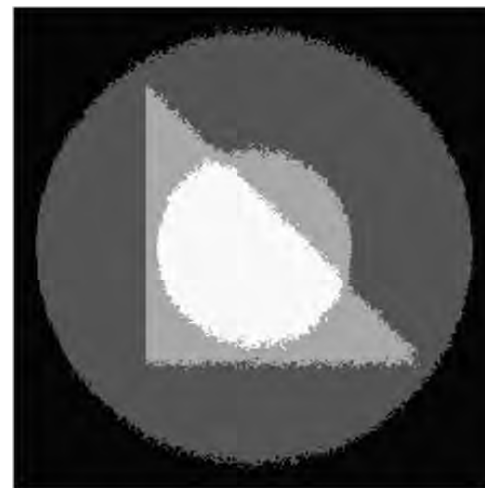
Four-phase Segmentation: Noisy and blurry image



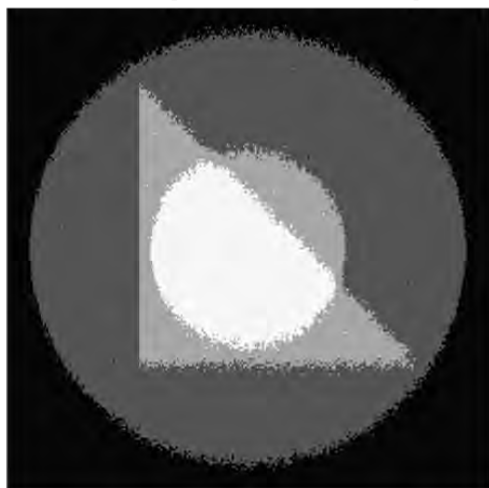
Noisy & blurry



Yuan *et al.* (10)



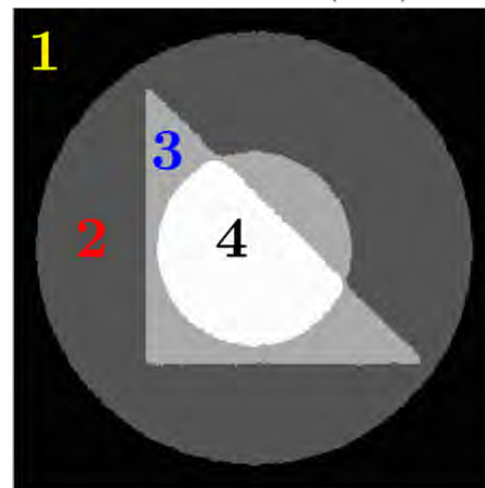
Li *et al.* (10)



Sandberg *et al.* (10)



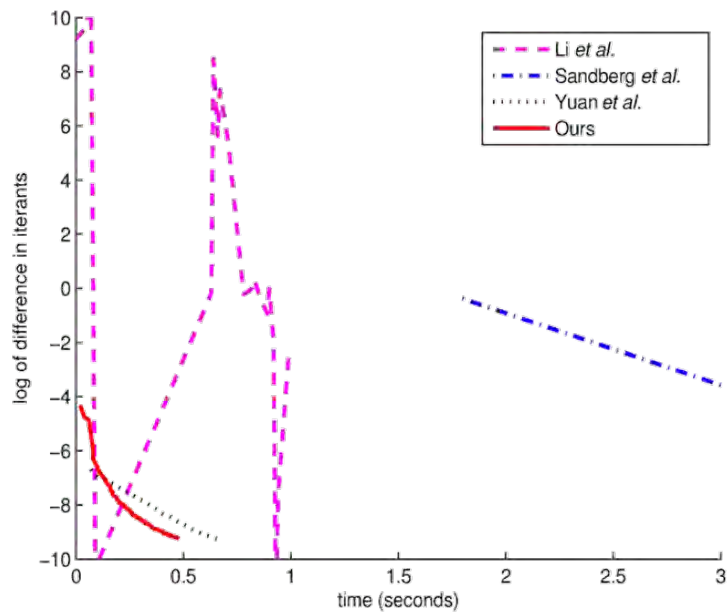
Steidl *et al.* (12)



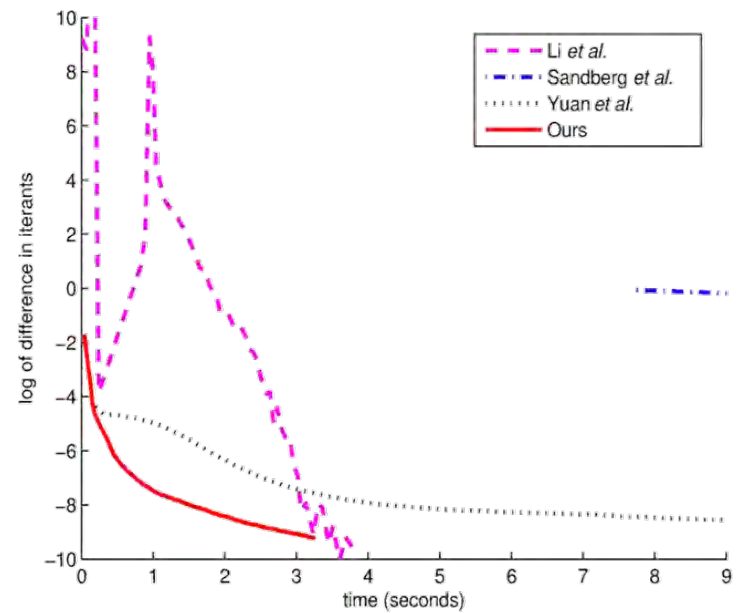
Our 4 phases from \hat{g}
using K-means ρ_i

Convergence History

Log of difference in iterates versus CPU time



Three-phase image



Four-phase noisy image

Our method is very **stable**.

CPU Time

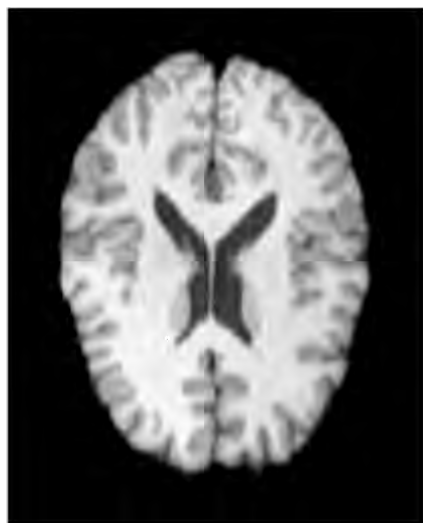
Multiphase: iteration numbers and CPU time in second

Example	Li (10)		Sandberg (10)		Yuan (10)		Our method	
	iter.	time	iter.	time	iter.	time	iter.	time
3-phase	100	1.56	2	3.15	32	0.58	62	0.57
4-phase	100	7.64	12	90.59	134	14.51	112	3.04
4-phase-blur	100	7.26	13	93.79	57	5.82	78	2.90

Our method is the **best** and **fastest** for multiphase segmentation.

Cai, C., and Zeng, *A two-stage image segmentation Method using a convex variant of the Mumford-Shah model and thresholding*, SIAM J. Imag. Sci. (2013).

Real MRI Brain Image with CPU Timing

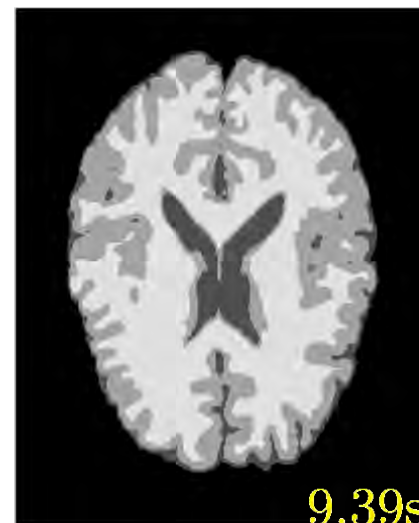


MRI brain image



12.23s

Yuan *et. al.* (10)



9.39s

Li *et. al.* (10)



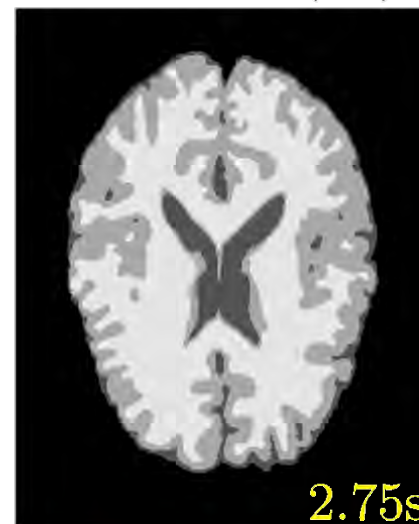
56.21s

Sandberg *et. al.* (10)



63.64s

Steidl *et. al.* (12)



2.75s

Our using ρ_i^K

1. Mumford-Shah Model
2. Our Two-stage Image Segmentation Method
3. Experimental Results
4. Extensions to Other Noise Models
5. Conclusions

Poisson and Multiplicative Gamma Noises

□ Poisson noise: observed image $f(x)$ follows

$$p_{f(x)}(n; g(x)) = \frac{(g(x))^n e^{-g(x)}}{n!}$$

with mean $g(x)$.

□ Multiplicative Gamma noise: $f = g \cdot \eta$ where $\eta(x)$ follows:

$$p_{\eta(x)}(y; \theta, L) = \frac{1}{\theta^L \Gamma(L)} y^{L-1} e^{-\frac{y}{\theta}} \text{ for } y \geq 0.$$

with mean 1 and variance of $\frac{1}{L}$.

Two-stage Method:

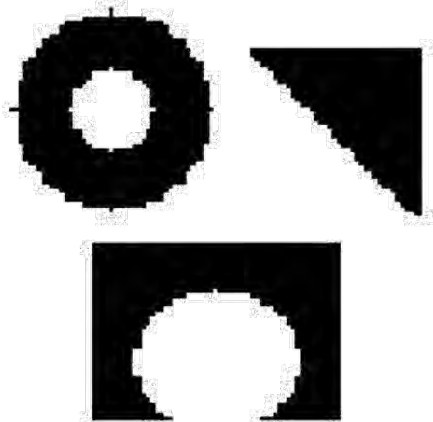
First stage: given f , solve

$$\min_g \left\{ \lambda \int_{\Omega} (\mathcal{A}g - f \log \mathcal{A}g) dx + \frac{\mu}{2} \int_{\Omega} |\nabla g|^2 dx + \int_{\Omega} |\nabla g| dx \right\}.$$

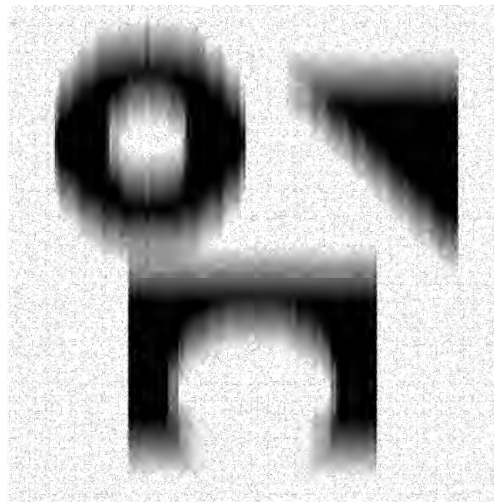
- data fitting term good for Poisson noise from MAP analysis
- also suitable for Gamma noise (Steidl and Teuber (10))
- objective functional is convex (solved by Chambolle-Pock)
- admits unique solution if $\text{Ker}(\mathcal{A}) \cap \text{Ker}(\nabla) = \{0\}$.

Second stage: threshold the solution \hat{g} to get the phases.

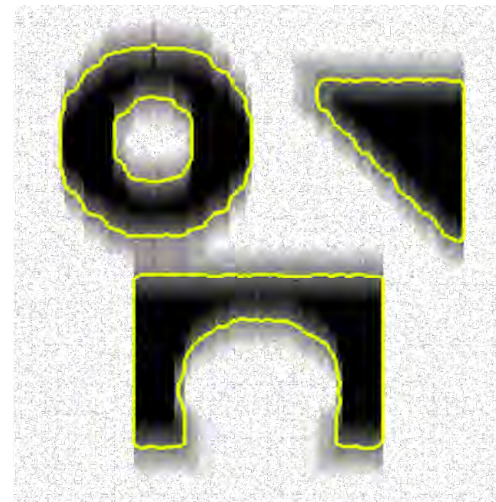
3-object Image with Poisson Noise and Motion Blur



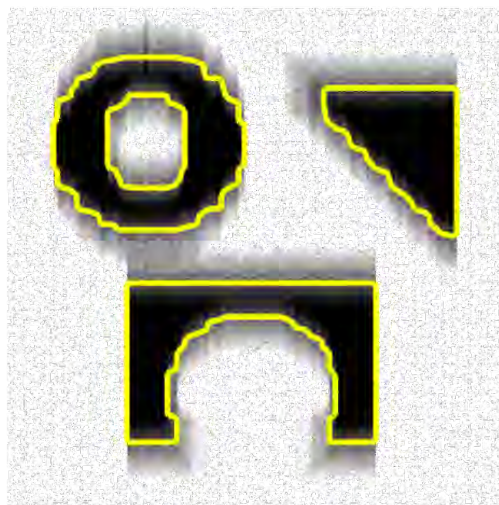
Original image



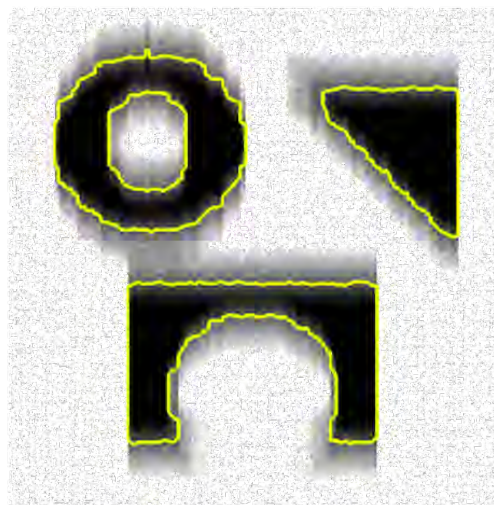
Noisy & blurred



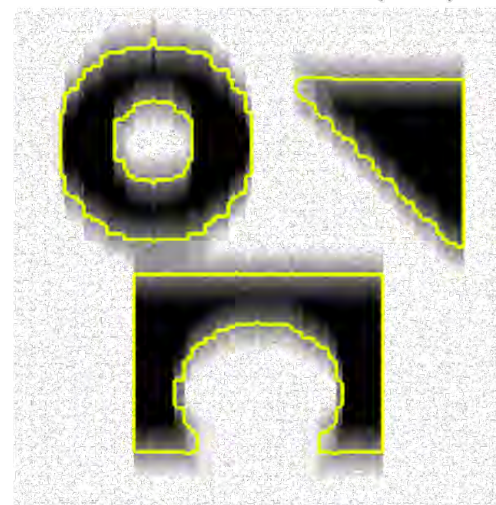
Yuan *et al.* (10)



Dong *et al.* (10)



Sawatzky *et al.* (13)



Our method

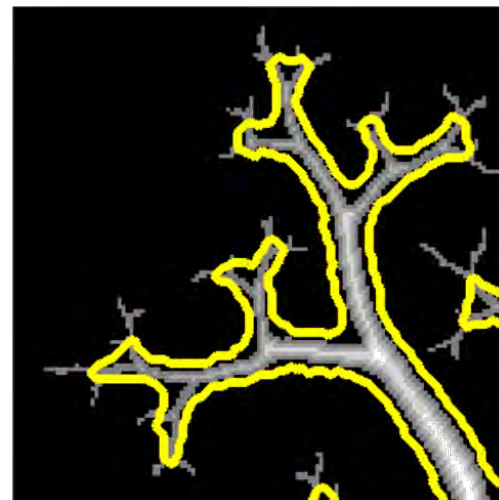
Tree with Gamma Noise with Gaussian Blur



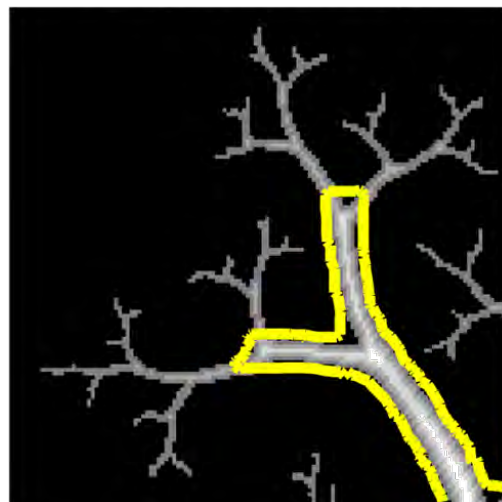
Original image



Noisy & blurred



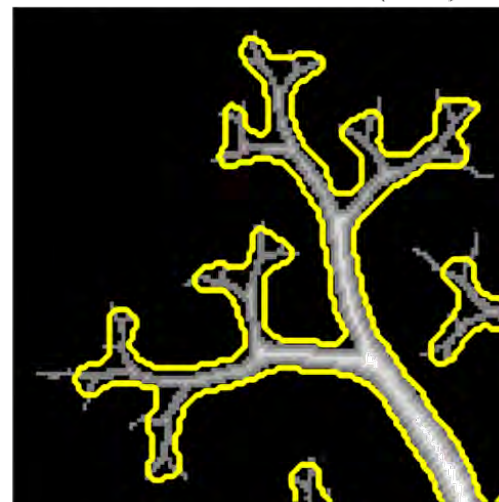
Yuan *et al.* (10)



Dong *et al.* (10)



Sawatzky *et al.* (13)

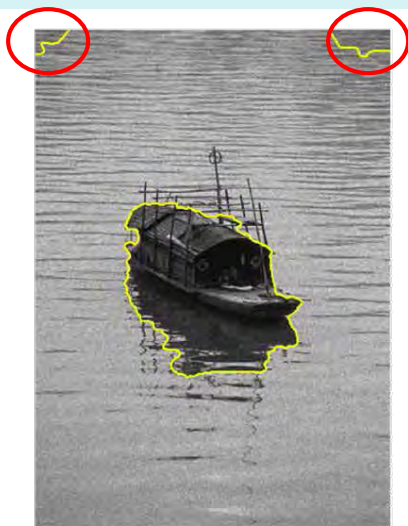


Our method

Boat with Poisson Noise



Noisy image



Yuan *et al.* (10)



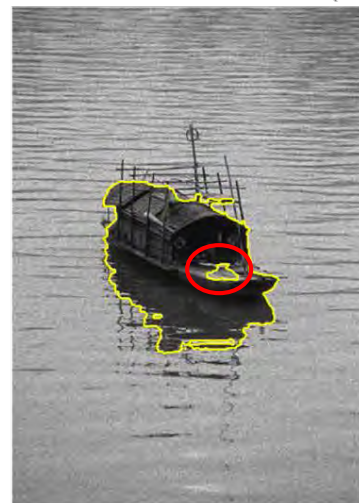
Dong *et al.* (10)



Sawatzky *et al.*
(13)

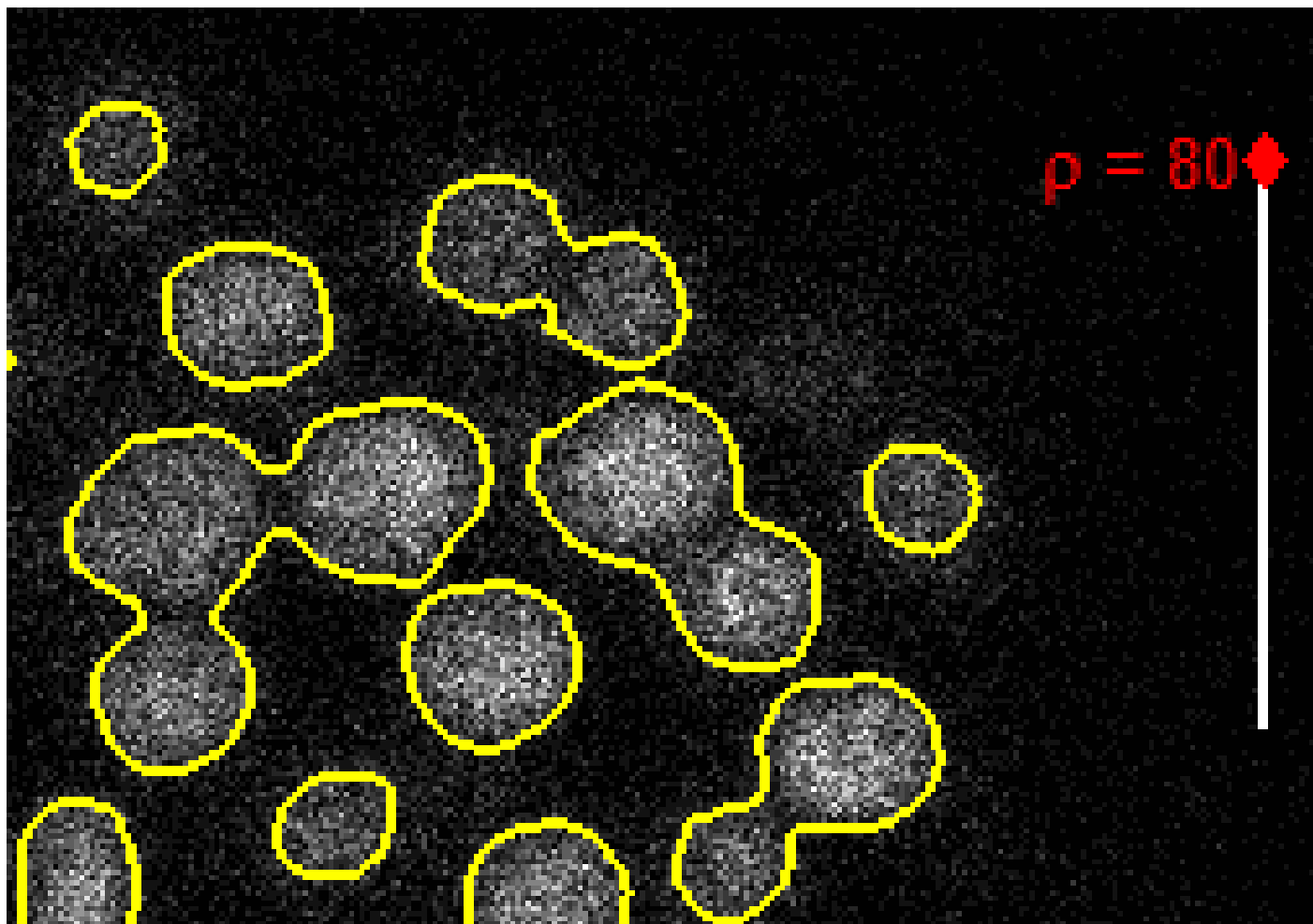


With $\mu = 0.05$,
 $\rho^K = 142$



With $\mu = 0$,
 $\rho^K = 104$

Segmentation Changes with Threshold



Real cell image from an automated cell tracking system.

CPU Time

2-phase: iteration numbers and CPU time in second

Test	Yuan*		Dong*		Sawatzky		Our method	
	iter.	time	iter.	time	iter.	time	iter.	time
3-Object	22	0.17	500	40.7	13	37.2	325	4.1
Tree	39	4.1	500	190.6	14	660.1	263	18.9
Boat	54	2.1	500	189.6	13	324.5	61	1.5
Anti-mass	51	5.1	500	138.0	9	137.8	80	3.2
Cells	46	6.4	500	255.5	17	1546.2	101	6.3
Bacteria	51	5.1	500	189.6	12	548.7	74	3.9

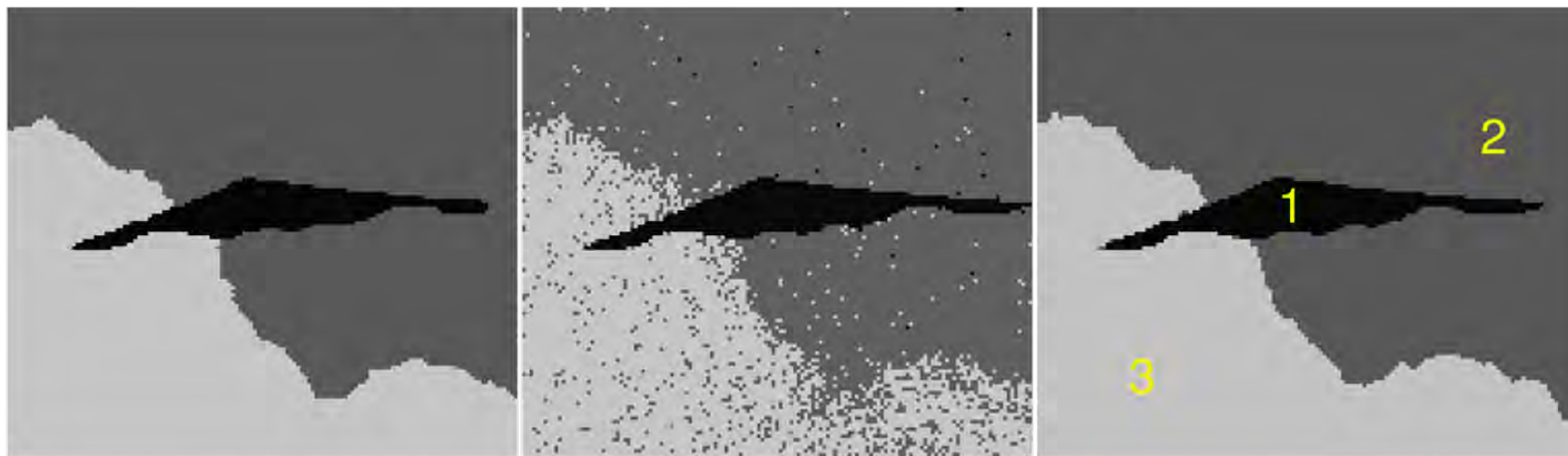
* Yuan's and Dong's algorithms were applied on images after Anscombe transformation.

Airplane with Multiplicative Gamma Noise



Original image

Noisy image

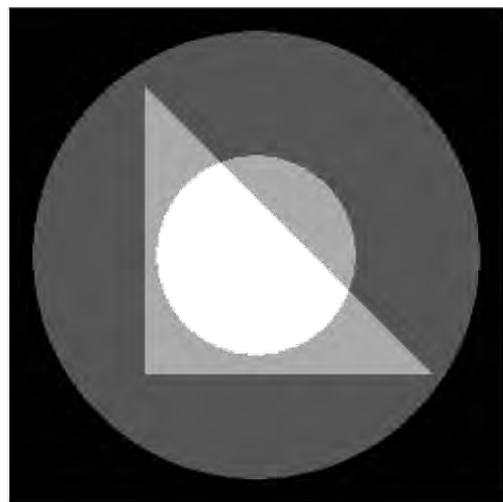


Yuan *et al.* (10)

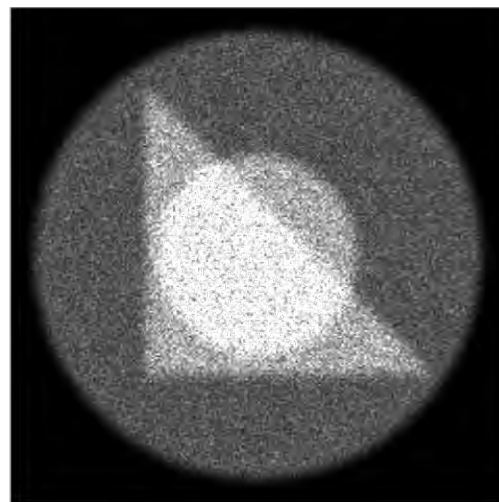
Li *et al.* (10)

Our method with ρ_i^K from K-means

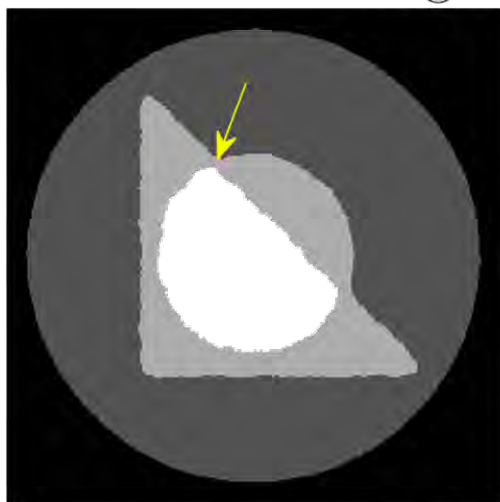
4-phase under Gamma Noise with Gaussian Blur



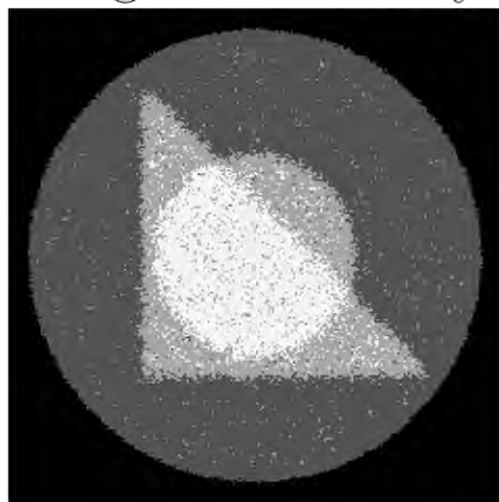
Original image



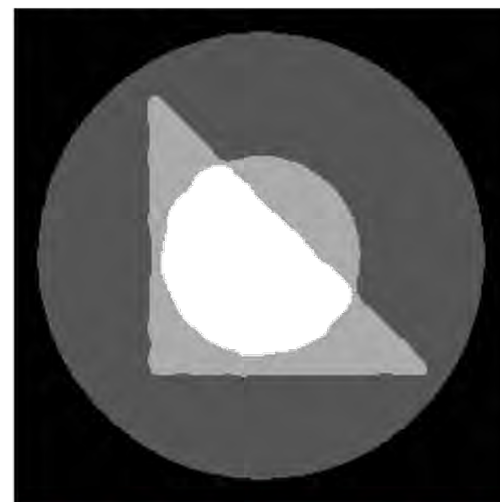
Noisy & blurred



Yuan *et al.* (10)

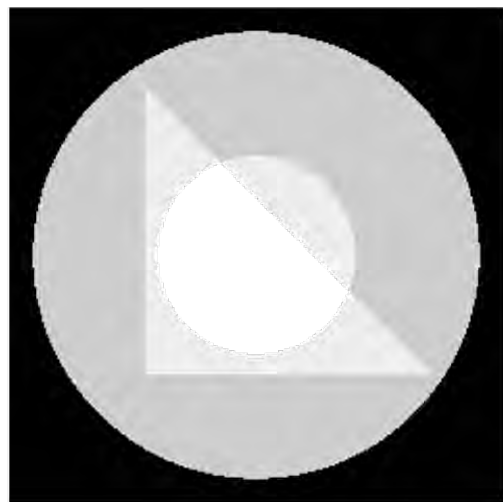


Li *et al.* (10)

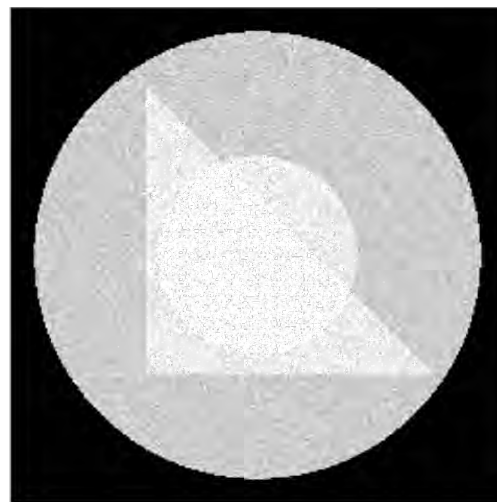


Our method with
 ρ_i^K

4-phase with Close Intensity under Poisson Noise

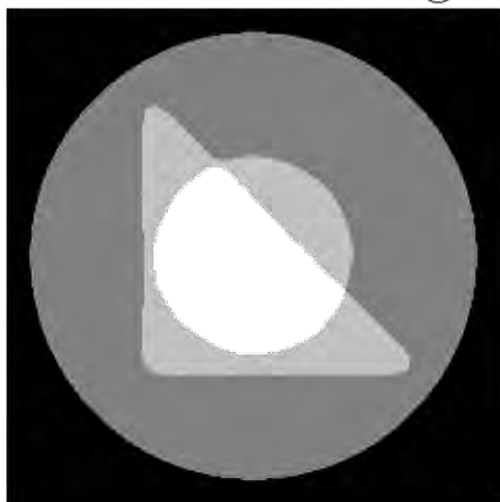


Original image



Poisson noise

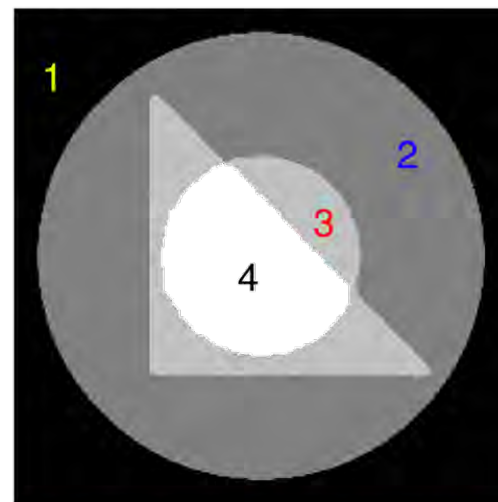
intensities of segmented images enlarged to reflect the details.



Yuan *et al.* (10)



Li *et al.* (10)

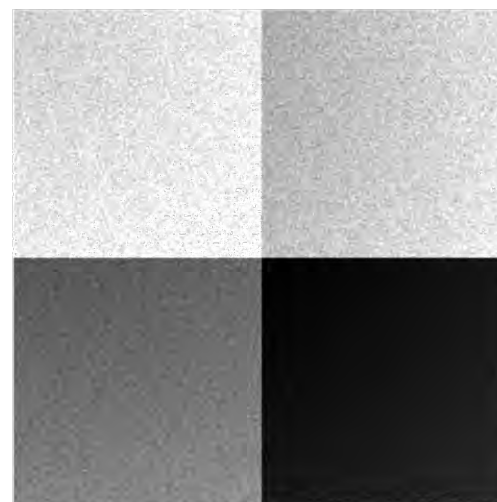


Our method with ρ_i^K

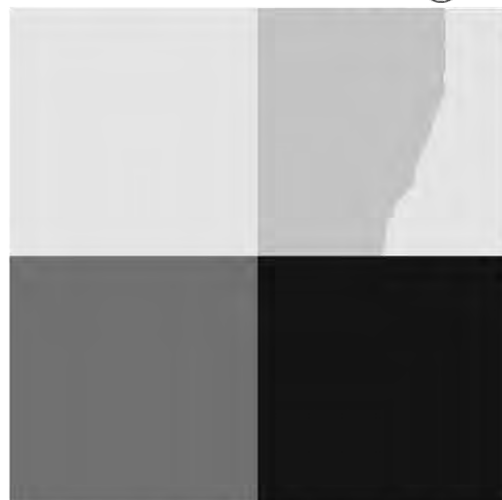
Image with Close and Varying Intensities



Original image



Poisson noise



Yuan *et al.* (10)

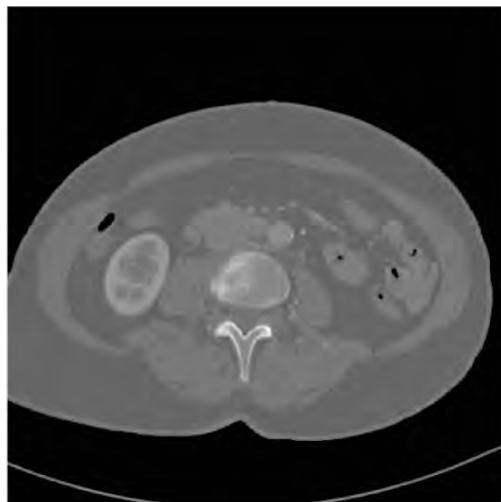


Li *et al.* (10)

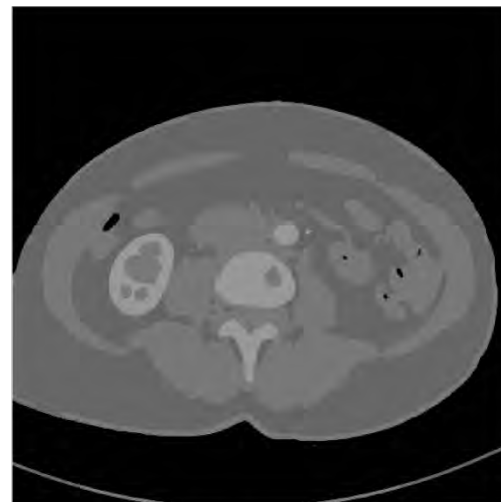


Our method with ρ_i^K

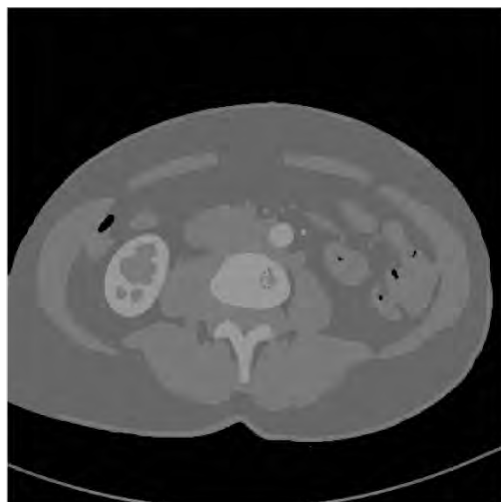
Real MRI Image



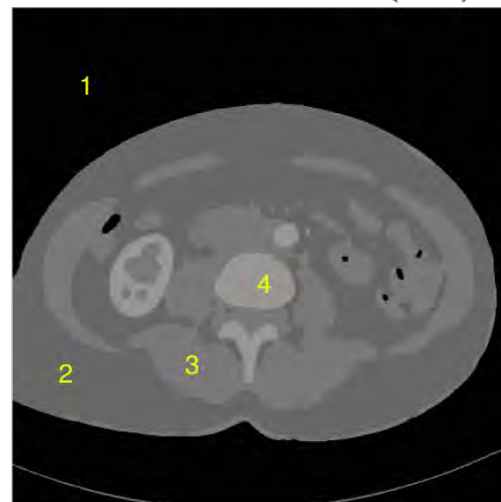
Original image



Yuan *et al.* (10)



Li *et al.* (10)



Our method with ρ_i^K

CPU Time

Multi-phase: iteration numbers and CPU time in second

Test	Yuan		Li		Our Method	
	iter.	time	iter.	time	iter.	time
Airplane	127	1.0	95	1.0	86	0.2
4-phase	57	2.2	49	1.6	184	2.3
Close-intensity	34	1.8	110	4.0	84	0.5
Varying-intensity	114	4.4	332	9.9	444	3.0
MRI	76	25.7	114	26.4	19	0.6

C., Yang, and Zeng, *A two-stage image segmentation method for blurry images with Poisson or multiplicative Gamma noise*, Accepted by SIAM J. Imag. Sci.

- 1. Mumford-Shah Model**
- 2. Our Two-stage Image Segmentation Method**
- 3. Experimental Results**
- 4. Extensions to Other Noise Models**
- 5. Conclusions**

Relationship with Image Restoration

Convex M-S Energy
 $E(g)$

$$\frac{\lambda}{2} \int_{\Omega} (f - \mathcal{A}g)^2 dx$$

$$\frac{\mu}{2} \int_{\Omega} |\nabla g|^2 dx$$

$$\int_{\Omega} |\nabla g| dx$$

ROF Model (1992)

Rudin, Osher and Fatemi

staircase

reduce by introducing
higher-order derivative:

T. Chan (00), Lysaker (03),
Steidl (08), Bredies (10),
Hintermüller (10), etc.

Relationship with Image Restoration

Convex M-S Energy
 $E(g)$



$$\frac{\lambda}{2} \int_{\Omega} (f - \mathcal{A}g)^2 dx$$

+

$$\frac{\mu}{2} \int_{\Omega} |\nabla g|^2 dx$$

+

$$\int_{\Omega} |\nabla g| dx$$



Hintermüller (2010): image restoration model

ROF + Thresholding = Chan-Vese

Solve ROF model in the 1st stage:

$$\min_g \left\{ \frac{\lambda}{2} \int_{\Omega} (f - g)^2 + \int_{\Omega} |\nabla g| \right\}$$

for \tilde{g} . Then threshold \tilde{g} properly in the 2nd stage.

One can get a 2-phase segmentation (Σ, c_1, c_2) which satisfies the Chan-Vese model:

$$\min_{\Sigma, c_1, c_2} \left\{ \frac{\mu}{2} \int_{\Sigma} (f - c_1)^2 + \frac{\mu}{2} \int_{\Omega \setminus \Sigma} (f - c_2)^2 + \text{Length}(\partial\Sigma) \right\}$$

□ See [Cai & Steidl, EMMCVPR, 2013]

□ $\text{Length}(\Gamma) \approx \int_{\Omega} |\nabla g|$

Conclusions

- Look for **smooth** solutions of Mumford-Shah model
- **Convex** segmentation model with **unique** solution
—can be solved easily and fast
- Model solved **only once**—no need to solve the model again when threshold or number of phases changes
- Easily **extendable** to blurry images and non-Gaussian noise
- Link **image segmentation** and **image restoration**

References

- X. Cai, R. Chan, S. Morigi, and F. Sgallari, Vessel segmentation in medical imaging using a tight-frame based algorithm, *SIAM J. Imaging Sci.*, (2013).
- X. Cai, R. Chan, and T.Y. Zeng, A two-stage image segmentation method using a convex variant of the Mumford-Shah model and thresholding, *SIAM J. Imaging Sci.* (2013).
- R. Chan, H.F. Yang, and T.Y. Zeng, A two-stage image segmentation method for blurry images with Poisson or multiplicative Gamma noise, *Accepted by SIAM J. Imag. Sci.* (2013).

URL: www.math.cuhk.edu.hk/~rchan

Happy 75th Birthday Bob!



Welcome to Hong Kong



SIAM Conference on
IMAGING SCIENCE



Tom Goldstein and Stanley Osher, SIAM J. Imaging Sciences, Vol.2, No.2

May 12-14, 2014
Hong Kong Baptist University
Hong Kong

and Chinese University of Hong Kong



Thank you!